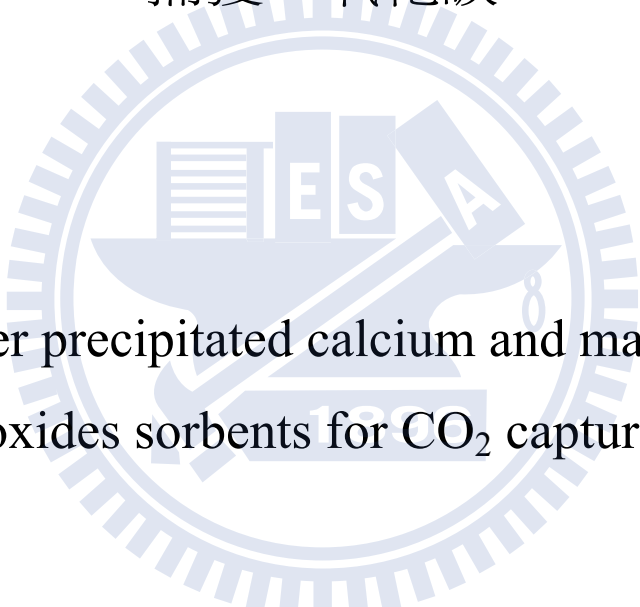# 國立交通大學環境工程研究所

碩士論文

利用海水沉澱法所製備之碳酸鈣與碳酸鎂捕獲二氧化碳

Sea water precipitated calcium and magnesium oxides sorbents for CO$_2$ capture

研 究 生：Rosa Amarilis Dubón Mazariegos

指導教授：白曛綾教授

民 國 九 十 九 年 十 月

利用海水沉澱法所製備之碳酸鈣與碳酸鎂捕獲二氧化碳

Sea water precipitated calcium and magnesium oxides sorbents for CO_2 capture

研 究 生 :杜若思　　Student：Rosa Amarilis Dubón Mazariegos

指導教授:白曛綾　Advisor：Hsunling Bai

國 立 交 通 大 學

環 境 工 程 研 究 所

碩 士 論 文

A Thesis

Submitted to Institute of Environmental Engineering

College of Engineering

National Chiao Tung University

In Partial Fulfillment of the Requirements for the Degree of

Master In Environmental Engineering

October 2010

Hsinchu, Taiwan, Republic of China

中華民國九十九年十月

ACKNOWLEDGMENT

Sea water precipitated calcium and magnesium oxides sorbents for CO_2 capture

Student: Rosa Dubón   Advisor: Hsunling Bai

Institute of Environmental Engineering

National Chiao Tung University

Abstract

Calcium based sorbent for cyclic calcination/carbonation is considered as one of the promising CO_2 capture technologies. But the prevention of CaO sintering and deterioration is a challenge for the development of CaO technology. In the present study the mechanical mixing method between sea water precipitated CaO and MgO to enhance the sorption capacity during cyclic capture is demonstrated. The cyclic CO_2 capture capacities of the sorbents were evaluated by thermo gravimetric analysis (TGA). The results indicated that by adding only 5 wt. % of MgO into the CaO sorbent (CaO-MgO), the CO_2 absorbed amount can be improved by 17% compared to the original CaO sorbent. Instead of passing CO_2 only during the sorption period, passing CO_2 right after the calcination process is completed (i.e. during the cooling and sorption periods) can greatly improve the capacity and stability of the cyclic absorption. The heating and cooling rates also affect the sorbent performance significantly.

Keywords: CO_2 capture and storage (CCS), greenhouse gas, greenhouse effect, limestone, calcium oxide, chemical looping.
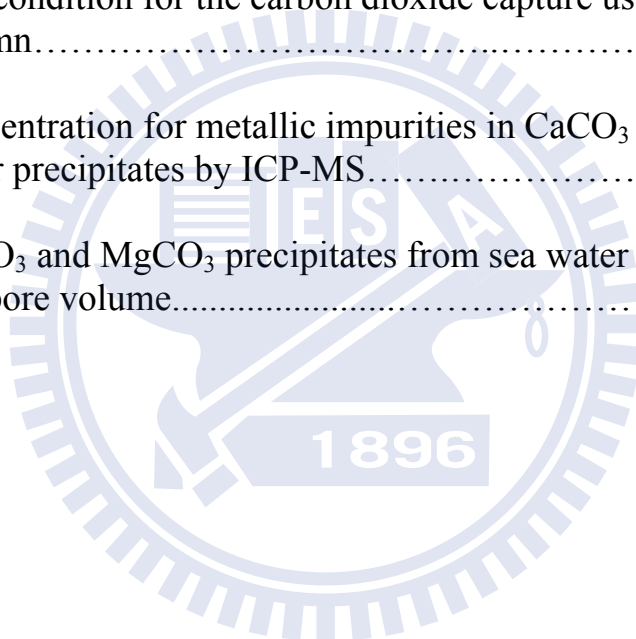
CONTENT

LIST OF TABLES

LIST OF FIGURES

CHAPTER ONE INTRODUCTION

1.1 Research background

In recent years it has been claimed that the human activity, especially the use of fossil fuel energy, is responsible for the increasing CO_2 concentrations in the atmosphere affecting climate change (IPCC 2005). It was stated that the upper limit of safe greenhouse gas concentration is somewhere between 300-350 ppm CO_2 (Hansen 2008). Carbon dioxide emission is currently 385 ppm and rising at a rate of 2 ppm per year, means that actions needed to 'draw down' atmospheric CO_2. Therefore reducing the CO_2 emission is considered to be one of the most important challenges of this century. Theoretically, CO_2 (or carbon) Capture and Storage (CCS) has the ability to meet this challenge and reduce CO_2 atmospheric concentration.

The main purpose of CCS is to reduce CO_2 emissions by capturing CO_2 that is released from large point source emitters such as power plants, refineries, cement plants and steel mills. The CO_2 must then be store in depleted oil and gas reservoirs or deep saline formations that have the geological characteristics necessary to store large quantities of CO_2. This will allow the continued use of coal, oil, and gas while avoiding the CO_2 emissions currently associated with fossil fuel use.

Many researchers agree (Fang et al 2009a; Gupta and fan 2002; Abandes and Alvarez 2003) that in terms of CO_2 capture, the utilization of naturally occurring Ca-based sorbents, such as limestone and dolomite, which are plentiful, cheap, and widely available, are suitable for the CO_2 separation process. However, their CO_2 capture capacity decreases during multiple carbonation/calcination reaction cycles.

The calcium looping cycle uses $CaCO_3$ as a CO_2 carrier via the reversible reaction:

$$CaO_{(s)} + CO_{2(g)} \rightleftharpoons CaCO_{3(s)}$$
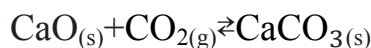
This extracts CO_2 from the exhaust stream and provides a pure stream of CO_2 suitable for sequestration. The decline in sorbent capability during multiple carbonation-calcination cycles, leading to a loss of reversibility, is a key issue in all such processes. The ultimate utilization determines the sorbent make-up rate required in any commercial plant, heavily influencing the cost of operation (Abanades et al. 2004). Also different applications have been proposed (Johnsen et al. 2006; Han and Harrison 1994; Lin et al. 2001), including CO_2 removal from steam reformers, gasifiers, and water-gas shift reactors where the carbonation reaction can improve hydrogen yields while also providing heat and facilitating CO_2 sequestration.

Limestone is one of the highest potential sorbents. Due to its low costs, wide availability, relatively high activity and high temperature requirements which allow heat integration with power plants or heat demanding processes (Romeo et al. 2009). The study of Feng et al. (2007) indicated that limestone also has favorable thermodynamic properties in comparison to other metal oxides.

Stoichiometrically, 56 g of CaO should react with 44 g of CO_2 to form 100 g of $CaCO_3$. This translates to a CO_2 capture capacity of about 0.786 g of CO_2/g of CaO. However, the performance of all reported CaO-based absorbents deteriorates as the number of carbonation-decarbonation cycles increases. This is caused by absorbent sintering during the highly exothermic carbonation process. Owing to these facts, enhancing the durability of CaO-based CO_2 absorbents has

been an active research topic for many years. As a result two major approaches have been tested: (1) incorporation of inert materials, such as MgO, (Albrecht et al. 2008a; Li et al. 2009) and Al_2O_3 (Feng et al. 2006; Li et al. 2006), (2) modification of the stability Lu et al. (2009) and structure of CaO (Gupta and Fan 2002).

1.2 Motivation

Based on the fact that is necessary to find out good absorbents for the CO_2 capture, this research is focused on the study of $CaCO_3$ precipitates from sea water for the dry absorption of carbon dioxide as well as finding a method for the production of CaO-MgO sorbents without the problem of loss-in-capacity after multiple carbonation/calcination cycles.

One of the challenges in the development is the prevention of sintering of the sorbent which causes the CO_2 capture capacity of the material to deteriorate rapidly after a few cycles of utilization. In this study a simple mixing method of calcium and magnesium carbonates precipitated from sea water is presented which can be a sintering-resistant sorbent.

The carbonation and calcination processes will be addressed by multi-cycle testing in order to assess the expected sorbent life time using thermo gravimetric analysis (TGA). These sorbents are provided by Power Research Institute, Taiwan Power Company.

1.3 Objectives

The objectives of this study are listed in the following:

1. Determine the suitable conditions for the CO_2 absorption process using $CaCO_3$ precipitates from sea water as a precursor of the CaO using TGA system.

2. To find a method to produce a CaO/MgO mixed sorbent for enhancing the absorption capacity and improving durability through a calcination/carbonation cycles.

3. To analyze the characteristics of the fresh and regenerated sorbents in order to find the causes of the deterioration of the sorbents.
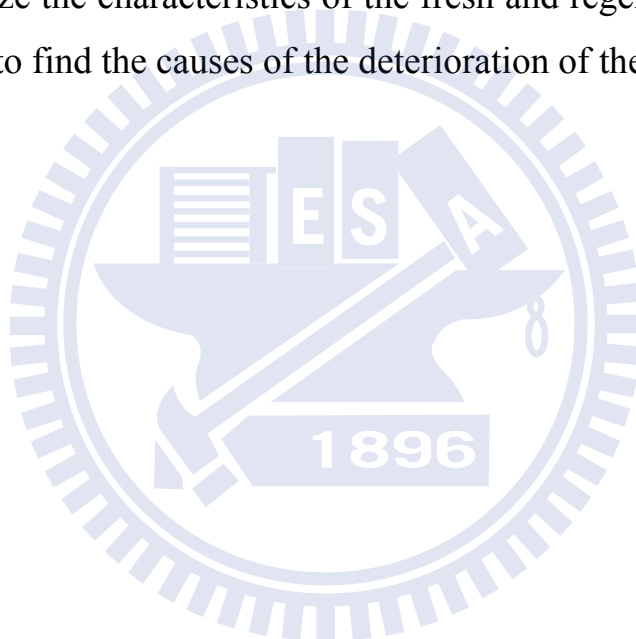
CHAPTER TWO LITERATURE REVIEW

2.1 System to capture CO_2

A wide range of technologies exists for separation and capture of CO_2 from gas streams. Current commercial processes employ a variety of physical and chemical mechanisms including absorption, adsorption, membranes and cryogenics (Hendriks 1994; Mimura et al. 1997).

The choice of a suitable technology depends upon the characteristics of the CO_2-laden gas stream, which in turn depends mainly on the type of power plant technology. There are four basic systems for capturing CO_2 from use of fossil fuels and/or biomass (IPCC 2005) .

- Capture from industrial process streams
- Pre-combustion capture
- Post-combustion capture
- Oxy-fuel combustion capture

2.1.1 Capture from industrial process streams

Current examples of CO_2 capture from process streams are purification of natural gas and production of hydrogen-containing synthesis gas for the manufacture of ammonia, alcohols and synthetic liquid fuels. Most of the techniques employed for CO_2 capture in the examples mentioned are also similar to those used in pre combustion (IPCC 2005).

2.1.2 Pre combustion capture

The technology for pre-combustion can be widely applied in fertilizer, chemical, gaseous fuel (H_2, CH_4), and power production. In these cases, the fossil fuel is partially oxidized, such as in a gasifier. The resulting syngas (CO and H_2) is shifted into CO_2 and more H_2, and then the resulting CO_2 can be captured from a relatively pure exhaust stream. The H_2 can now be used as fuel; the carbon is removed before combustion takes place.

Figure 2-1 shows the pre combustion system, which involves several steps. At the beginning the air separator removes nitrogen from the air that is pumped into the unit, the remaining product is an almost pure stream of oxygen. In the gasifier the coals with oxygen and steam form a "syngas". Then the syngas is then passes through the first filtering process, where small "fly ash" particles are removed. The shift reactor injects steam, causing a chemical reaction that converts the CO into hydrogen (H_2) and carbon dioxide (CO_2). Next, sulphur is removed from the syngas. In CO_2 the syngas stream is passed though a CO_2 capture device such as a CO_2 absorber, which captures the CO_2 from the gas stream. For CO_2 sorbent/solvent processes the sorbent is moved to the desorber to be "regenerated". Regeneration in the CO_2 desorber generally involves heating the sorbent, which releases the CO_2 ready for compressing and transporting. Once the CO_2 has been removed, the syngas consists primarily of hydrogen.   This is then used to power gas turbines to generate electricity. In the heat recovery stage, the excess heat from the combustion of the syngas is captured to generate steam and this in turn is used to power a steam turbine which also generates electricity. At the end of the process, the residual water vapour and air is released into the atmosphere (Miliband 2009).
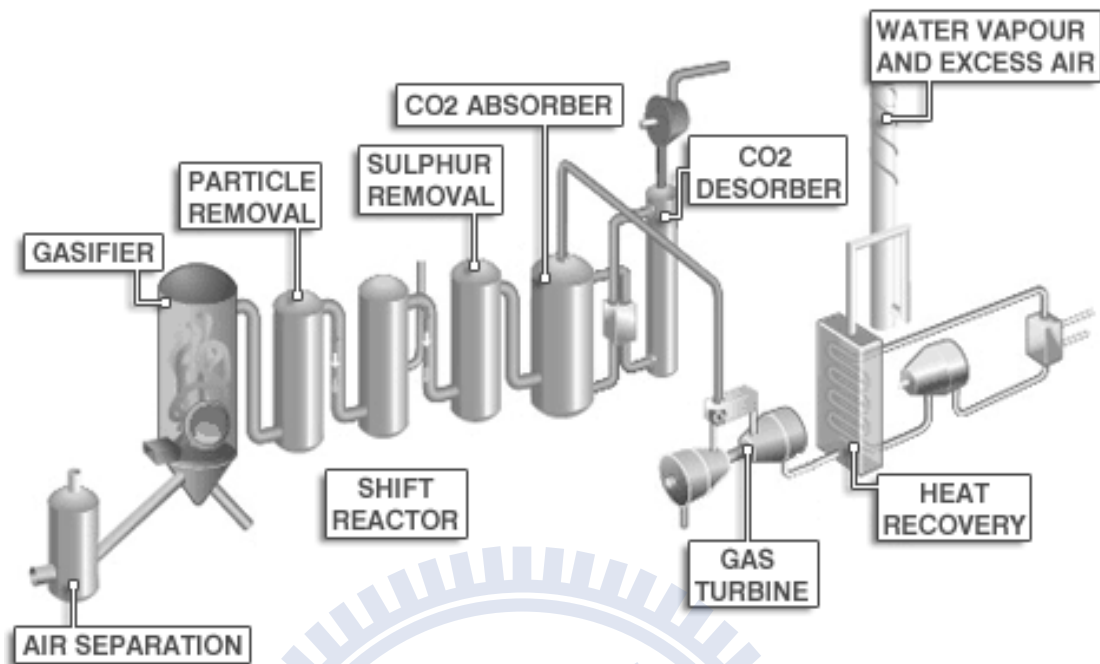
Figure 2-1 Pre combustion system for CO_2 capture (Vattenfall 2008)

2.1.3 Post combustion capture

In post-combustion, the CO_2 is removed after combustion of the fossil fuel; this is the scheme that would be applied to conventional power plants. Instead of being discharged directly to the atmosphere, flue gas is passed through equipment which separates most of the CO_2 (IPCC 2005). The CO_2 is fed to a storage reservoir and the remaining flue gas is discharged to the atmosphere.

Figure 2-2 shows the diagram of the post combustion system, first in the fuel injection stage, the coal is washed and pulverized before entering into boiler. The heat generated from the combustion of the coal/air mixture in the boiler creates steam, which is then pumped to the turbine. The turbines generate electricity, which is transmitted into the distribution grid. Once the steam has passed through the turbine, it arrives at a condenser, this unit uses cool water to condense the steam back into

water, allowing it to be piped back into the boiler and be re-heated again.

The particle removal is the first of several cleaning processes that the flue gas will pass through. The stage of sulphur removal involves a process called flue gas desulphurization (FGD). Before the flue gas enters the CO_2 absorber, it needs to be cooled. In this stage, using water lowers the temperature of the gas. In the CO_2 absorber, the gas stream is passed though a CO_2 captured by a device, typically an absorber, which reacts with the CO_2. Then after purged from the flue gas, the almost pure stream of CO_2 can now be compressed into a liquid state (Miliband 2009).
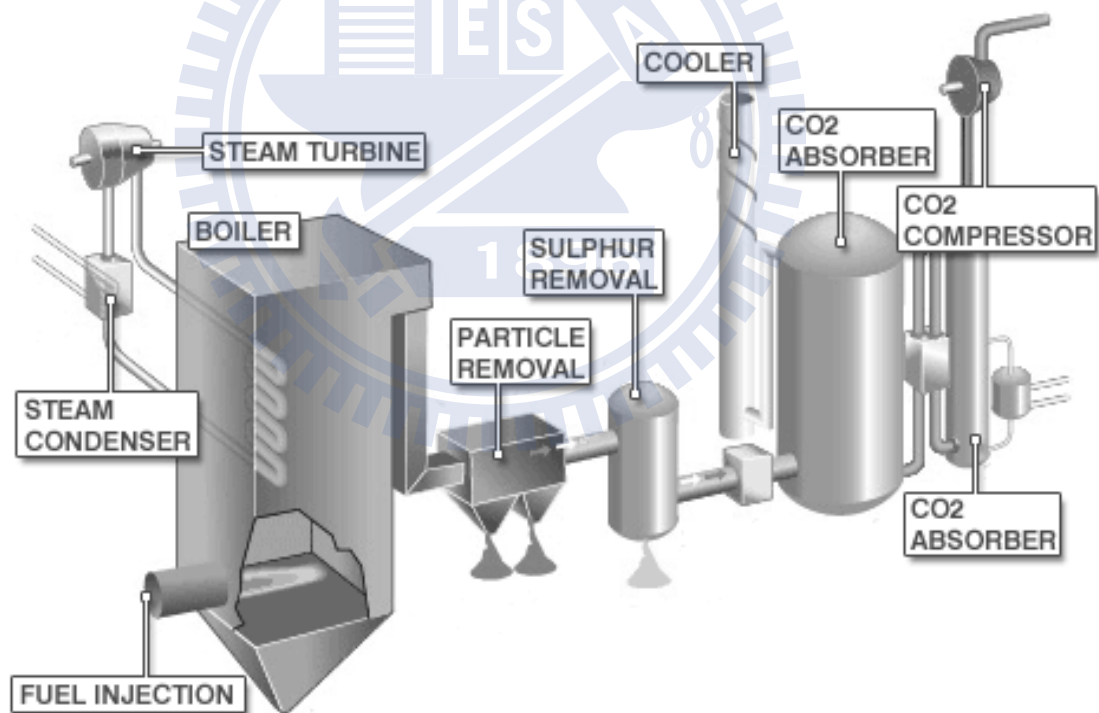
Figure 2-2 Post combustion system for CO_2 capture (Vattenfall 2008)

2.1.4 Oxy fuel combustion capture

In oxy-fuel combustion, nearly pure oxygen is used for combustion instead of air, resulting in a flue gas that is mainly CO_2 and H_2O. If fuel is burnt in pure oxygen, the flame temperature is excessively high, but CO_2 and/or H_2O-rich flue gas can be recycled to the combustor to moderate this. Oxygen is usually produced by low temperature (cryogenic) air separation and novel techniques to supply oxygen to the fuel, such as membranes and chemical looping cycles are being developed (IPPC 2005).
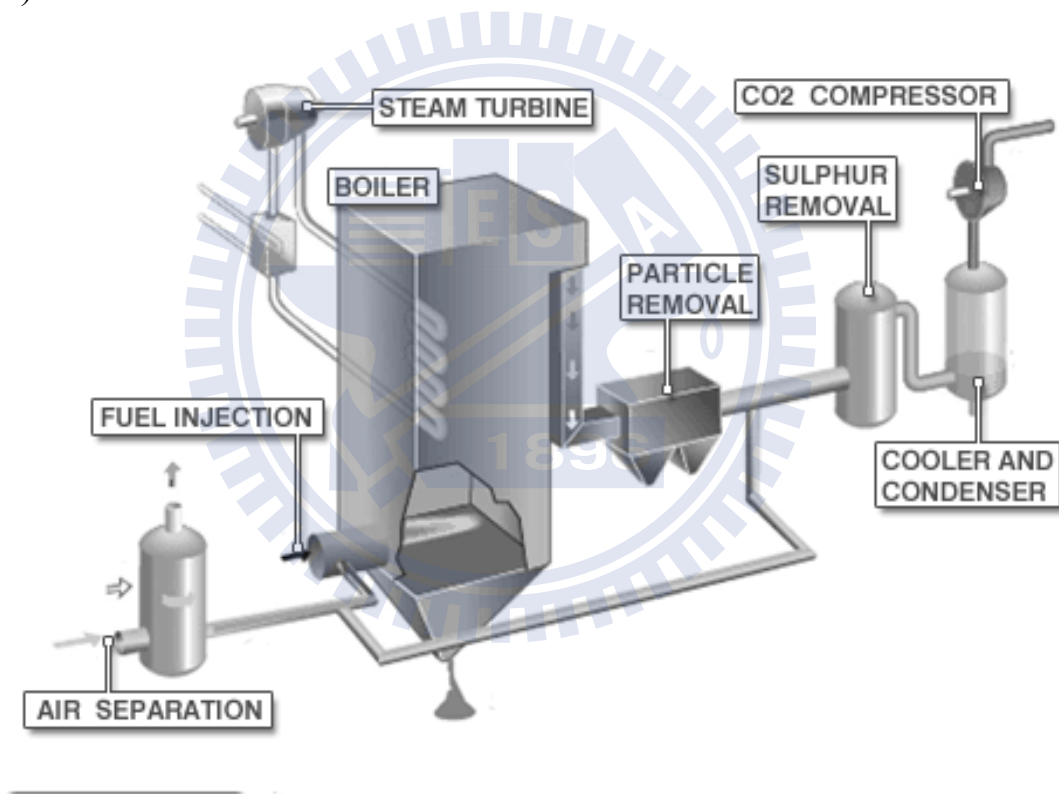
Figure 2-3 Oxyfuel combustion system for CO_2 capture (Vattenfall 2008)

Figure 2-3 shows the oxyfuel combustion system that involves burning the coal in nearly pure oxygen rather than the air/coal mix currently used in conventional power plants.

2.2 Types of CO_2 capture technologies

CO_2 capture systems use many of the known technologies for gas separation which are integrated into the basic systems for CO_2 capture (IPCC 2005).

- Separation with sorbents/solvents
- Separation with membranes
- Distillation of a liquefied gas stream and refrigerated separation

Figure 2-4 shows the general schemes of the main separation processes relevant for CO_2 capture. The gas removed in the separation may be CO_2, H_2 or O_2. Figure 2-4 (a) governs many important CO_2 capture systems, including leading commercial options like chemical absorption and physical absorption. In Figures 2-4 (b) and (c) one of the separated gas streams (A and B) is a concentrated stream of O_2, H_2 or O_2 and the other is a gas stream with all the remaining gases in the original gas (A+B).
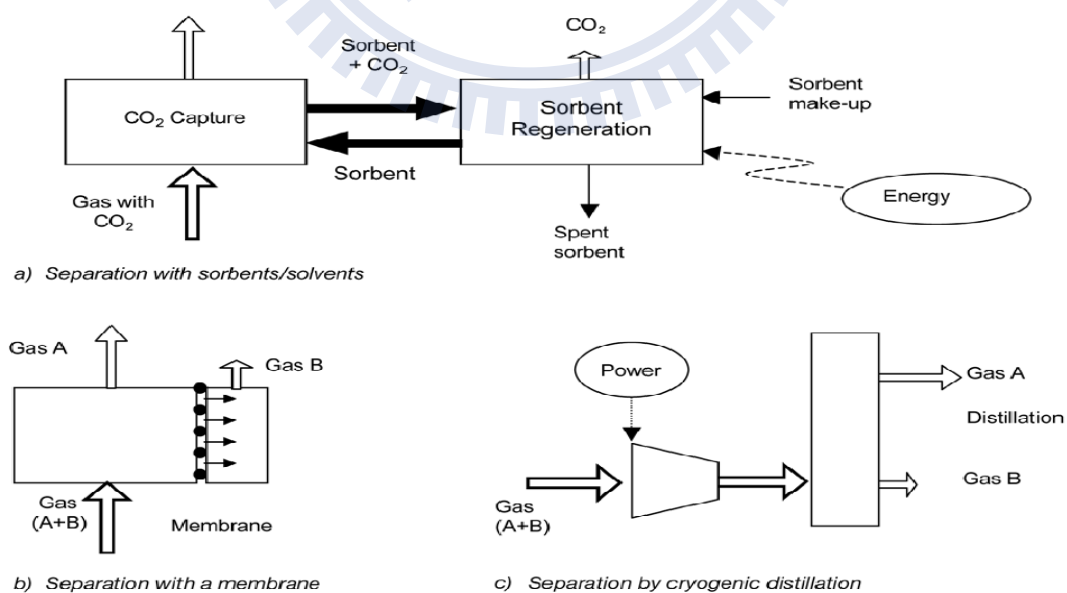
Figure 2-4 Types of CO_2 capture technologies. (IPPC 2005)

2.2.1 Separation with sorbents/solvents

The separation process is achieved by passing the CO_2-containing gas in intimate contact with a liquid absorbent or solid sorbent that is capable of capturing the CO_2. The sorbent is loaded with the captured CO_2 and it is being transported to a different vessel, where it releases the CO_2 (regeneration) after being heated, after the pressure decrease or after any other change in the conditions around the sorbent. After the regeneration step the sorbent is sent back to capture more CO_2 in a cyclic process (ICCP 2005).

- Solvents

    Mono-ethanolamine (MEA) is a widely used amine for CO_2 capture. CO_2 recovery rates of 98% and product purity in excess of 99% can be achieved.

- Sorbents

    Solid adsorbents, such as zeolites and activated carbon, can be used to separate CO_2 from gas mixtures. There are various techniques employed for CO_2 separation includes pressure swing adsorption (PSA), vacuum pressure swing adsorption (VPSA) and thermal (or temperature) swing adsorption (TSA). In PSA, CO_2 adsorbed on the surface is released by lowering the bed pressure. In VPSA, vacuum is applied to further pull the CO_2 out of the bed. The regeneration cycles are short (usually requiring a few seconds). In TSA, the saturated bed is heated to release the adsorbed CO_2.

2.2.2 Separation with membranes

The membrane gas absorption process makes use of porous, water-repelling membranes for the transfer of components between a gas and a liquid (Gabelman and Hwang 1999). These Components are diffused through the pores and are absorbed by a suitable liquid. In the membrane absorber CO_2 is chemically bound in an aqueous solution and it is removed from the rich solution using thermal regeneration, using strip gas or vacuum. The lean solution is then fed back to the membrane absorber where it is reused.

2.2.3 Distillation of a liquefied gas stream and refrigerated separation

A gas can be made liquid by a series of compression, cooling and expansion steps. Once in liquid form, the components of the gas can be separated in a distillation column. In the case of air, this operation is currently carried out commercially on a large scale (IPCC 2005).

2.3 Modes of CO_2 storage

The storage of CO_2 can be achieved with different methods, which include gaseous storage in various deep geological formations, liquid storage in the ocean, and solid storage by reaction of CO_2 with metal oxides to produce stable carbonates as is shown in Figure 2-5.

There are several generic modes of geological CO_2 storage, including:

- Depleted oil and gas reservoirs
- Deep saline aquifer formation

- Storage in association with CO_2 enhanced oil Recovery (EOR) projects
- Coalbed formation
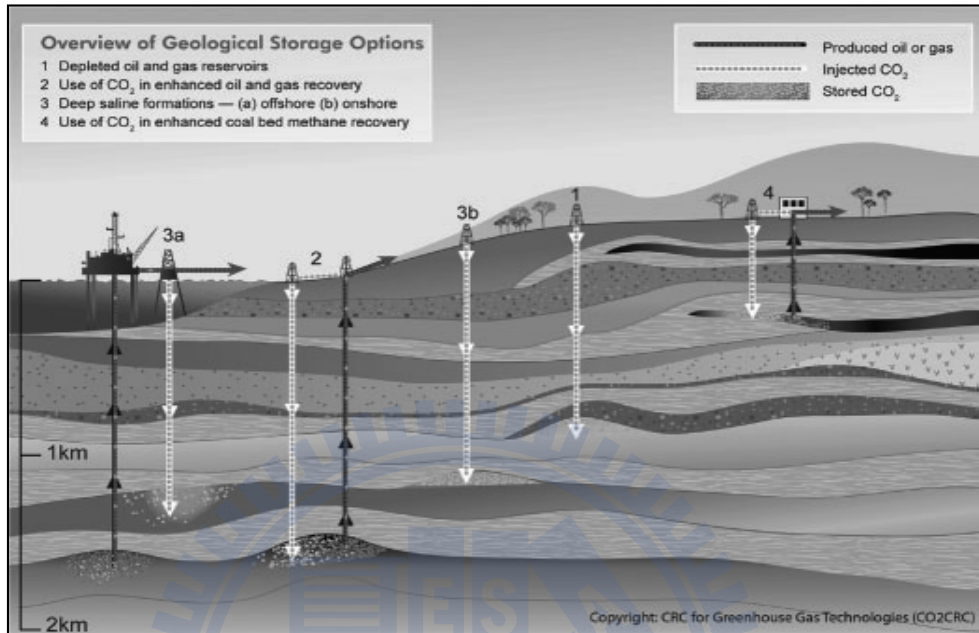
Figure 2- 5 Overviews of geological storage options.   (IPCC 2005)

2.4 CO_2 utilization

Carbon dioxide is a valuable industrial gas with a large number of uses which include production of chemicals, such as urea, refrigeration systems, inert agent for food packaging, beverages, welding systems, fire extinguishers, water treatment processes, horticulture, precipitated calcium carbonate for the paper industry and many other smaller-scale applications (IPCC 2005).

Much of the carbon dioxide used commercially is recovered from synthetic fertilizer and hydrogen plants, using either a chemical or physical solvent scrubbing system. Other industrial sources of CO_2 include the fermentation of sugar (dextrose) used to produce ethyl alcohol:

$$C_6H_{12}O_6 \rightarrow 2C_2H_5OH + 2CO_2.$$

13

2.4.1   New process for CO_2 abatement

There are new processes for CO_2 abatement which include:

- Organic chemicals and polymers

    A number of possible new process routes for the production of chemicals and polymers have been considered in which CO_2 is used as a substitute for other C1 building blocks, such as carbon monoxide, methane and methanol.

- Fuel production using carbon dioxide

    Liquid carbon-based fuels, gasoline and methanol for example, are attractive because of their high energy density and convenience of use, which is founded in part on a well established infrastructure. Carbon dioxide could become the raw material for producing carbon-based fuels with the help of additional energy. Methanol production is an example of the synthesis of liquid fuels from CO_2 and hydrogen, the producing reactions which are exothermic, take place over a copper/zinc/alumina catalyst at about 260°C as is reported by different authors (Inui et al. 1998; Halmann and Steinberg 1999; Arakawa 1988).

2.4.2   Capture of CO_2 in biomass (plants and algae)

Biomass production of fuels also falls into the category of generating fuels from CO_2. With the help of photosynthesis, solar energy can convert water and CO_2 into energetic organic compounds like starch. These in turn can be converted into industrial fuels like methane, methanol, hydrogen or biodiesel (Larson 1993).

    Biomass also can be produced in natural or agricultural settings, or in industrial settings, where elevated concentrations of CO_2 from the

off-gas of a power plant would feed micro-algae designed to convert CO_2 into useful chemicals (Benemann 1997).

2.4.3 Mineral carbonation

Mineral carbonation is one of technologies utilizing CO_2, used to form carbonated materials by the reaction between CO_2 and Ca or Mg-bound compounds such as wollastonite ($CaSiO_3$), olivine (Mg_2SiO_4), and serpentine ($Mg_3Si_2O_5(OH)_4$) (Maroto et al. 2005). This technology can be also considered as an accelerated carbonation in terms of making the reaction shorter using high purity CO_2. One of advantages of this technology compared to other CO_2 storage technologies is that CO_2 is stably stored in final products such as $CaCO_3$ and $MgCO_3$.

2.5 Carbon dioxide capture sorbents

A variety of materials have been reported (Feng et al. 2007) to be able to absorb CO_2. These can be classified as follows:

- Microporous and Mesoporous Materials. These include carbon-based sorbents such as activated carbon, carbon fiber, and carbon molecular sieves, zeolites, and chemically or physically modified mesoporous materials such as MCM- 41.
- Metal Oxides. Many metal oxides exhibit carbonation and calcination reaction. However, a majority of these metal carbonates are thermally stable and calcined only at higher temperatures. The calcination temperatures of some metal carbonates ($CaCO_3$ ~750 °C, $MgCO_3$ ~385 °C, $ZnCO_3$ ~340 °C, $CuCO_3$ ~290 °C and $MnCO_3$ ~440 °C) are within the temperature range of interest (200-800 °C)

(Butt et al. 1996). Various metal oxides such as those listed in Table 2-1 have strong affinity to CO_2.

Table 2-1 CO_2 capacity of metal oxides (Feng et al. 2007)

Metal Oxide	CO_2 capacity (g of CO_2/g of oxide)
Ag_2O	0.189
BaO	0.287
CaO	0.785
Cs_2O	0.156
K_2O	0.468
Li_2O	1.471
MgO	1.092
Na_2O	0.709
Rb_2O	0.235
SrO	0.425
ZnO	0.54

- Hydrotalcite-like Compounds. These belong to a large class of anionic and basic clays, also known as layered double hydroxides (LDH). They are composed of positively charged brucite-like $(Mg(OH)_2)$ layers with trivalent cations substituting for divalent cations at the centers of octahedral sites of hydroxide sheet whose vertex contain hydroxide ions, and each -OH group is shared by three octahedral cations and points to the interlayer regions (Feng et al. 2007).

2.6   Absorption system to capture CO_2

Reaction-based processes can be used for separating CO_2 from flue gas. This process is based on the carbonation reaction in which gaseous CO_2 reacts with a solid metal oxide (represented by MO) to yield the metal carbonate (MCO_3) (Gupta & Fan 2002).

$$MO + CO_2 \rightarrow MCO_3$$
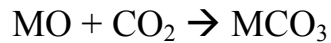
Once the metal oxide has reached its ultimate conversion, it can be thermally regenerated to the metal oxide and CO_2 by heating the metal carbonate beyond the calcination temperature. The calcination reaction can be represented by

$$MCO_3 \rightarrow MO + CO_2$$

There are two types of adsorption systems determined by IEA (International Energy Agency) that have been widely studied (Gomes and Yee 2002; Takamura et al. 2001; Ishibashi et al. 1996; Diagne et al. 1995) PSA (Pressure Swing Adsorption) and TSA (Temperature Swing Adsorption).

In the PSA process, CO_2 gases are captured at higher pressure and released at lower pressure, this technology requires a vacuum unit for regeneration. Similarly, TSA process adsorbed CO_2 at lower temperature and desorbed by heating. One important economical factor in these technologies is strongly related to the ultimate adsorption capacity of the solvent/sorbent (quantified by kg CO_2/ton solvent or sorbent) and kinetics of the adsorption process. Higher equilibrium capacities allow lower sorbent/solvent requirement and handling; lower regeneration costs and therefore lower capital and operating cost.

2.7 Carbonation and calcination cycles in the CaO-CO₂ absorption process

Calcined lime (main component, CaO) can be used to capture CO_2 in the exhaust gas or in the reactor during the utilization of fossil fuels (Wang et al. 2009). That is, calcium oxide (CaO) absorbs CO_2 to yield calcium carbonate ($CaCO_3$), and the $CaCO_3$ is then thermally decomposed to CaO, releasing nearly pure CO_2 for sequestration. In fact, the heat for decomposing $CaCO_3$ can be supplied by combusting fossil fuels, such as coal and natural gas, in a calciner. These two reactions are showed as follow:

$$CaO_{(s)} + CO_{2\,(g)} \rightarrow CaCO_{3(s)} \quad \Delta H^0\,298 = -178 \text{ kJ/mol}$$
$$CaCO3(s) \rightarrow CaO(s) + CO_2\,(g) \quad \Delta H^0\,298 = 178 \text{ kJ/mol}$$
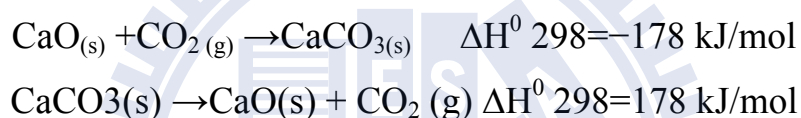
Specifying the conditions for a carbonation step must strike a balance between high temperatures which favor the speed of reaction, and low temperatures which favor the equilibrium conversion. Barker (1973) found that the carbonation reaction took place in two stages; an initial rapid rate was followed by a slower approach to a conversion plateau.

Both the limestone and dolomite react with CO_2 in these two stages. The initial carbonation stage is kinetically controlled with a fast reaction rate between CaO and CO_2. At this stage, the outlet CO_2 concentrations are not higher than 3% for a stable absorption period. After the stable absorption period, CO_2 concentrations abruptly increased and then increased very slowly, indicating that the CO_2 capture capacity of the CaO was nearly exhausted. Owing that large part of active CaO was converted to $CaCO_3$ and the carbonation stage moved to the second stage controlled by the diffusion in the product layer (Fang et al 2009b). During

the latter and slower stage of the reaction, it was found that CO_2 concentration does not affect the rate of the reaction if it is maintained much higher than the corresponding equilibrium concentration for that temperature.

Abanades and Alvarez (2003) reported that the maximum carbonation conversion decreased during the carbonation/calcination cycles due to the loss in the porosity associated with the small pores and the increase in the porosity associated with the large pores. The formation of a larger volume molar product ($CaCO_3$) compared to CaO led to the plugging of these pores thereby causing a loss in the active surface area. Figure 2-6 shows the concept of pore filling and plugging at the pore-mouths of these sorbent particles by $CaCO_3$ product layer, preventing the access of CO_2 to un-reacted CaO at the pore interiors.
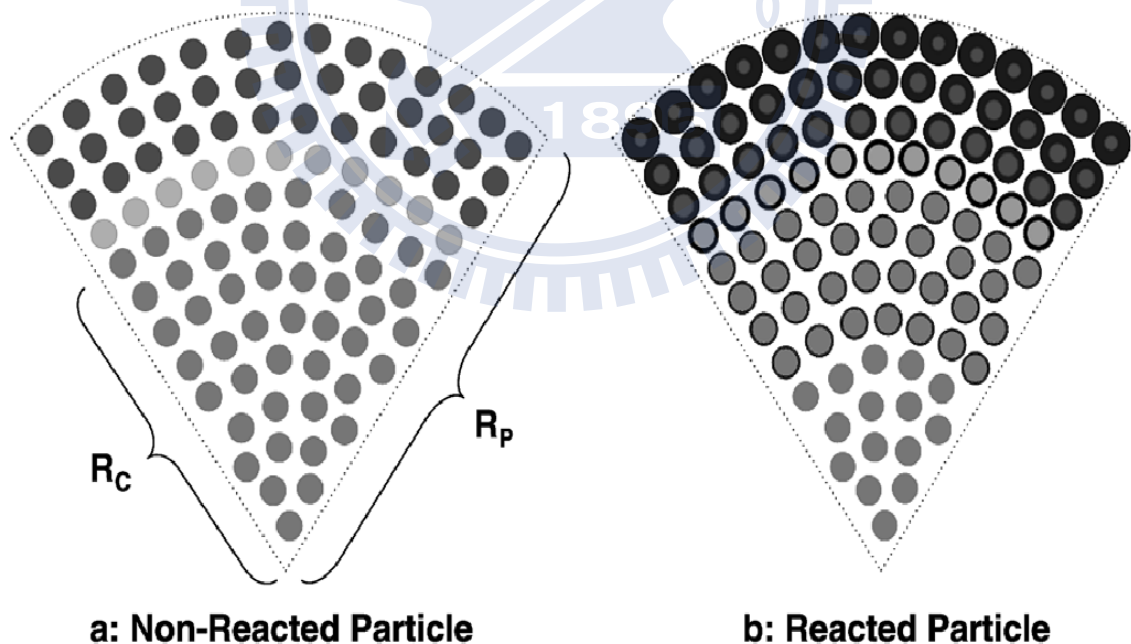
Figure 2-6 Non-reacted and reacted particle of $CaCO_3$ (Hassanzadeh and Abbasian2010)

The calcination reaction is favored by higher temperatures. The reactions proceed only if the partial pressure of CO_2 in the gas above the solid surface is less than the decomposition pressure of the $CaCO_3$. The latter pressure is determined by equilibrium thermodynamic considerations (Stanmore and Gilot 2005). A typical expression for equilibrium decomposition pressure P_{eq} (Silcox et al. 1989) is:

$$Peq = 4.137 \times 10^7 e^{\left(\frac{-20474}{T}\right)} atm$$

Figure 2-7 plots three of the expressions listed in the literature; the agreement is good except at lower temperatures. (Silcox et al. 1989; Hu and Scaroni 1996; Hartman and Tmka 2003).
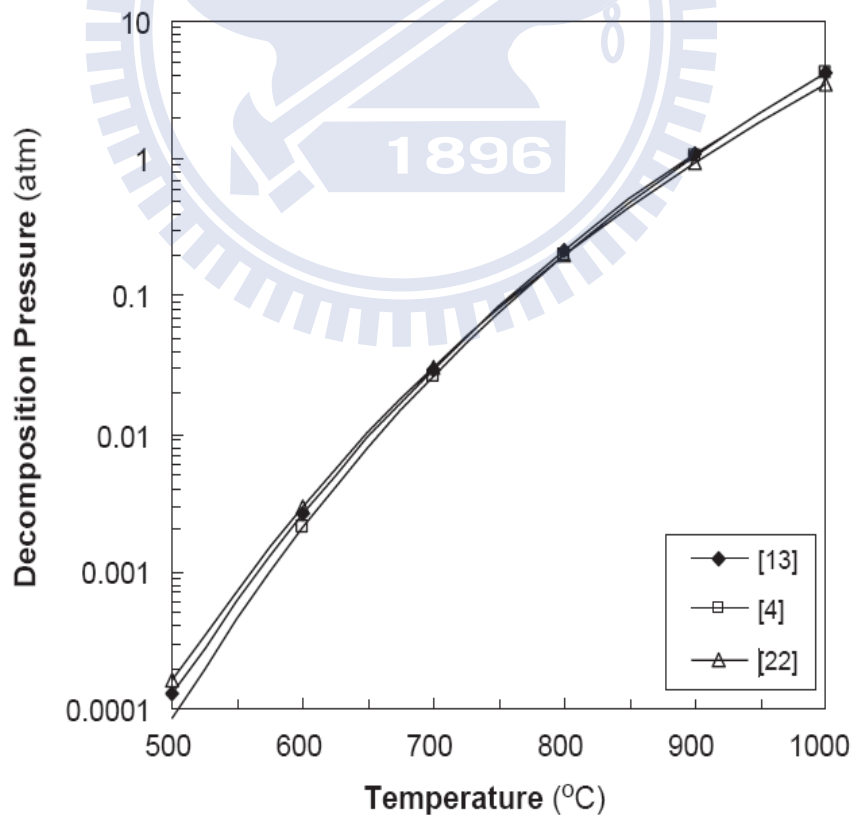
Figure 2-7 Decomposition pressure of carbon dioxide over calcium carbonate (Stanmore and Gilot 2005)

2.8   Sorbent deactivation

After the reaction of CaO with CO_2, the product $CaCO_3$ must undergo calcination to regenerate CaO for repeated use (Fang et al. 2009). In the calcination process, some pores are produced inside the CaO particle but, at the same time, CaO sintering occurs because of the high calcination temperature, which reduces the surface area and porosity with an increasing residence time. These two factors are very important for the reaction of CaO with CO_2, but sintering sharply reduces surface area and porosity, which strongly affects the CO_2 capture capacity and the reaction rates of CaO with CO_2.   As the number of carbonation/calcination sorbents already approach their lowest ultimate conversion, degradation is found to be more severe under more highly sintering calcination conditions at higher temperatures, higher residence times, higher partial pressures of CO_2 and H_2O.   Abanades and Alvarez (2003) indicated that for limestones, it appears that the reaction ceases when the product has built up to a depth of ~50 nm, averaged across the total surface area. Thus, the loss of surface area by sintering is a further contributing factor in the fall in sorbent capacity. However, there is still controversy surrounding the exact mechanism of deactivation.   Also Abanades et al. (2007) mentioned that the surface texture of cycled limestone commonly features shrinkage of smaller pores, usually accompanied by growing macro pores. These trends are typical of solid-state sintering in an intermediate stage (Randall and German 1996)   in which vacancies (or voids) generated by temperature-and-ion-sensitive lattice defects direct void volume from smaller to larger pores, whereas mass moves in the opposite direction.

2.9   Cost assessments

Freund (2003) estimated the costs for CO_2 transportation $1–$3/ t /100 km and sequestration ($4–$8)/t CO_2, these costs are small compared to the cost for CO_2 capture, estimated at $35– $55/t CO_2 capture (Abanades and Alvarez 2003). Singh (2003) indicated that the high cost of CO_2 capture is due to the considerable amount of energy required in the separation process. Therefore, reducing the cost of CO_2 capture is absolutely necessary to make CCS more economically attractive. However, the cost of sorbent must also be considered. Costs of limestone and dolomite are $26.7/ t and $30/ t, respectively (U.S. GPO 2005). Manovic and Anthony (2008) cited that synthesized sorbent with high performance and low cost would be highly beneficial for the CO_2 capture process using the carbonation/calcination cycle.

2.10   Magnesium carbonate

The reversible chemical reaction for CO_2 removal involving magnesium oxide is:

$$MgO + CO_2 \leftrightarrow MgCO_3 \qquad \Delta H \approx -96 \text{ kJ/mol}$$

Some reports suggest that high CO_2 absorption is possible only by chemisorptions of carbon dioxide molecules with metal oxide at higher temperatures (Song et al. 1998).   However Bhagiyalakshmi et al. (2010) found that the mesoporous MgO is highly basic with well-ordered pores to hold high CO_2 at lower and higher temperatures. The large surface active sites of mesoporous MgO initially holds the CO_2 molecules with smaller affinity and are trapped into the pores by chemical reaction of MgO and CO_2 to form $MgCO_3$.   It has been shown (Hassanzadeh and

Abbasian 2010) that the behavior of these materials is related to their lattice structure.

When the solid is porous in nature, the gaseous reactant diffuses into the interior pores of the particles and reacts with the active solid species at the surface of the pores. This can be described by the grain model, in which the solid particle is treated as an assemblage of numerous smaller grains. Surrounding these grains are macro-pores through which the gas has to diffuse to reach the grains. The reaction occurs at the surface of each grain, according to the un-reacted shrinking core model. As the reaction proceeds, the difference in the molar volumes of the solid product and the molar volume of the reactant results in an increase in the grain size. This decreases the pore volume between the grains, and also decreases the diffusion rate of the gaseous reactant through the sorbent particles.

At temperatures below the equilibrium temperature for carbonation of magnesium oxide (i.e. between 300 and 450 °C), the reactivity of the sorbent improves with increasing temperature, while at a higher temperature (i.e., 500 °C), because of the significant increase in the rate of reverse (i.e., regeneration) reaction, a decline in the sorbent reactivity is observed (Hassanzadeh and Abbasian 2010).

2.11 CaO sorbents mixed with other metals

It is believed that the capacity decay in CO_2 absorption process is mainly owing to the sintering of CaO and $CaCO_3$ (formed during carbonation) in the regeneration process, or the physical aggregation of the crystals leading to increased particle size, or reduced surface area of the produced CaO for the carbonation reaction in the next cycle. In order

to address this loss-in-capacity, many methods have been tested with varying degrees of success (Liu et al. 2010).

It has been reported (Li et al. 2009) that the method of incorporating the inert materials as MgO has a critical effect on the long term stability of the CaO-based absorbent. The investigation of Albrecht et al. (2008a) also showed that the rate of decline in CaO activity can be reduced by incorporating finely dispersed MgO in the sorbent. The absorption capacity of a limestone-based sorbent with 20 wt % MgO was 45% greater than that of a similar material without MgO by the end of the test, and the rate of decline in absorption capacity was very small.

In the study of Liu et al. (2010) a mixture of CaO and MgO was formed, in which during the regeneration of the CaO sorbent at 900 °C, the MgO particles, with a sintering temperature of 1289 °C, act as a physical barrier to prevent the sintering and aggregation of the $CaCO_3$ nano particles, which typically sinter at 527 °C. Therefore the high CO_2 capture capacity of the sorbent is maintained over a multitude of carbonation- regeneration cycles.

Chrissafis and Paraskevopoulos (2005) indicated that the degrading performance of CaO in cycles was mainly due to sintering, and by mixing high melting point compounds, such as Al_2O_3 or MgO, sintering may be inhibited to some extent. Li et al. (2009) reported a type of stable MgO-doped CaO absorbent, produced by mechanical mixing of small MgO particles with $Ca(CH_3COO)_2$, followed by high temperature calcination, gives as high as 53 wt % CO_2 capacity after 50 carbonation/decarbonation cycles. But without MgO addition the absorption capacity decrease to 26wt% for the 50th cycle under the same conditions. Some studies related to the enhancement of the sorbent for carbonation/calcination cycles can be found in Table 2-2.

Table 2-2 Performance of some Adsorbents for CO2 Capture (Li et al. 2009)

Materials	System	Conditions	Absorption Capacity	Reference
52 % CaO 67 % CaO 75 % CaO Calcium D gluconate monohydrate and Magnesium D-gluconate hydrate (as support)	TGA	Ads Tem 650 °C , 30 min. 15% CO_2, Des Tem 900 °C, 10 min 100%vN2.	0.39 CO_2g/g 0.50 CO_2g/g 0.56 CO_2g/g After 24 cycles.	(Liu et al. 2010)
MgO-doped CaO absorbents	TGA	Ads Tem 758 °C , 30 min.100% CO_2, Des Tem 900 °C, 30 min 100%v He	0.53 CO_2g/g After 50 cycles.	(L. Li et al. 2009)
PPC-CaO	TGA	Ads Tem 800 °C , 5 min.100% CO_2, Des Tem 950 °C, 5 min 100%v N_2	0.40 CO_2g/g After 50 cycles.	(Gupta & Fan 2002) (Gupta and Fan 2002)
Dolomite (Cao-MgO 1:1 Molar	TGA	Ads Tem 800 °C , 5 min.100% CO_2, Des Tem 950 °C, 5 min 100%v N_2	0.18 CO_2g/g After 50 cycles	(Nakawa and Ohashi 1998)
20 Wt% MgO doped CaO	TGA	Ads Tem 750 °C , 20 min.100% CO_2, Des Tem 750 °C, 30 min 100%v N_2	0.30 CO_2g/g After 50 cycles	(Albrecht et al. 2008)
Stabilized CaO nanoparticles	TGA	Ads Tem 700 °C , 300 min.100% CO_2, Des Tem 700 °C, 30 min 100%v N_2	0.39 CO_2g/g After 50 cycles	(H. Lu et al. 2009)

CHAPTER THREE   EXPERIMENTAL METHOD

3.1   Procedure and method

There are several parts involved in the operation of the experimental study: sorbent preparation, characterization of the samples, CO_2 sorption/desorption condition and systems procedures. Figure 3-1 shows the flow chart of this work.

3.2   Sorbent preparation technique

The sea water precipitated $CaCO_3$ and $MgCO_3$ sorbents were obtained from Power Research Institute, Taiwan (PRIT). A method permitting a selected production of calcium carbonate and magnesium carbonate precipitates was developed (Lan and Hong 2005) for the fixation of carbon dioxide by chemical precipitation it is described briefly as follows:

50 ml of 4 M sodium hydroxide solution and 20 ml of 2 M sodium carbonate solution were added to 1.8 L of sea water in a 2L flask. This mixture was magnetically stirred for about 30 min then allowed to settle for 4 hr. After that, three fourths of the supernatant sea water was considered to be provided by directly injecting carbon dioxide into the resulting sea water a flow rate of 1L/min for 48 hours. Sufficient amount of carbon dioxide was considered to provide by directly injecting carbon dioxide into the resulting sea water at flow rate of 1.0 L per minute for 48hrs. In this instance, calcium carbonate precipitates could be

exclusively separated from the suspended sea water by 0.45um membrane filtration. Magnesium carbonates precipitates, were produced by complete drying of the filtrate sea water, rinsed with de ionized water and dried.
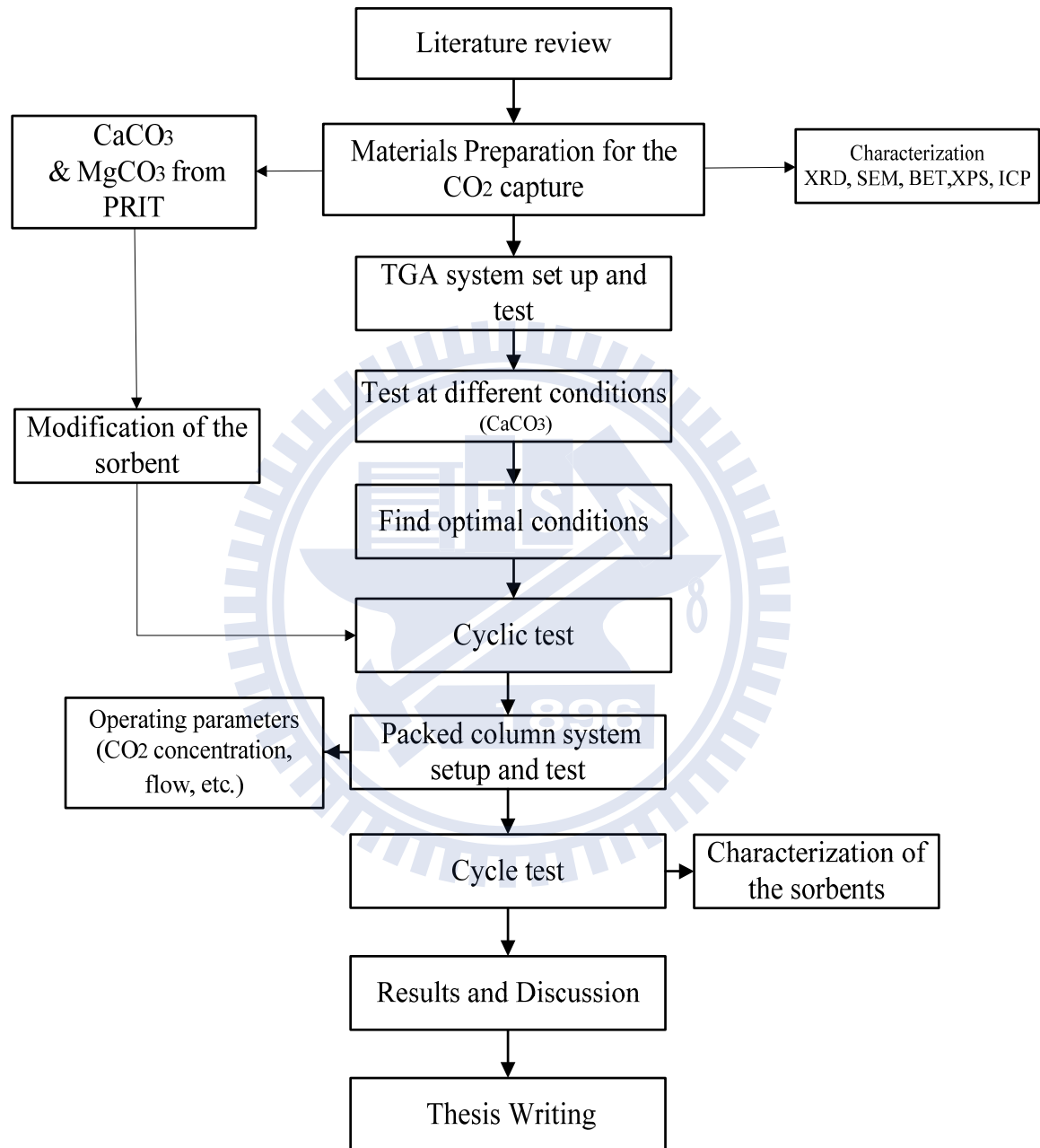
Figure 3-1 Flow chart of the experimental study

- Calcium and Magnesium Carbonate mixture

The mixture of calcium and magnesium carbonate for the production of an anti-sintering sorbent were prepared by the following procedure based on the study of Chen (2009). Appropriate amounts of calcium carbonate and magnesium carbonate were mixed with distilled water and methanol. The purpose of adding methanol was to dissolve the magnesium carbonate for better mixing.

The above mixture was vigorously stirred for 1 hour at 75°C, and then dried at 110°C overnight. After drying, the sample was ground into a fine powder.
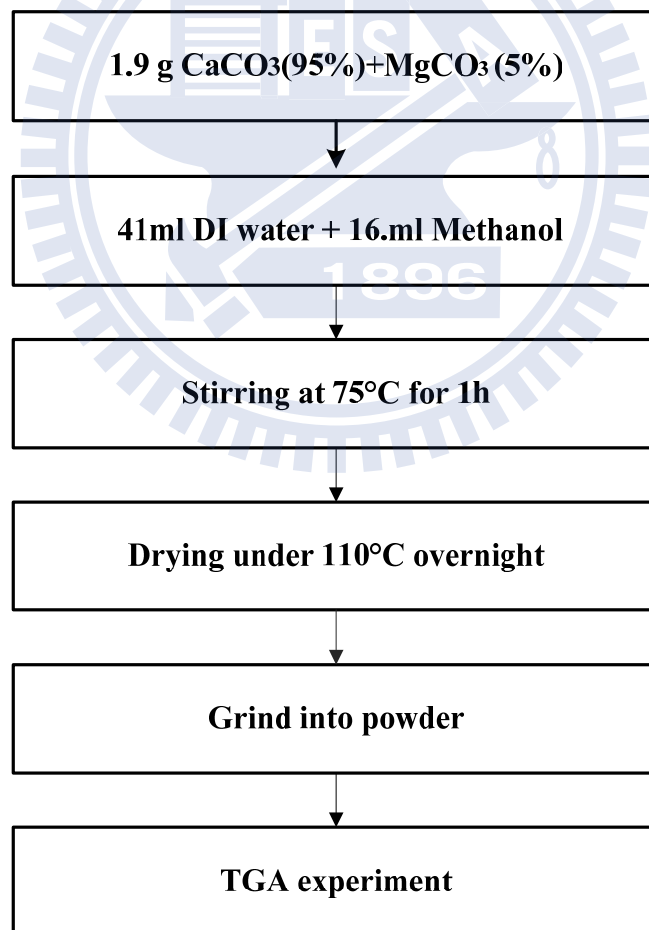
Figure 3-2 Calcium and Magnesium carbonate mixture procedure.

3.3 Characterization

Characterization of $CaCO_3$ and $MgCO_3$ were done by XRD, SEM, ICP-MS and BET surface area measurements. These tests were performed in order to study the chemical and physical composition, and the morphology of the samples.

- X-ray Powder Diffractometer (XRPD)

  $CaCO_3$ and $MgCO_3$ were characterized by X-ray diffraction (XRD) patterns on a D/MAX-RB diffract meter using Cu KR radiation (λ) 1.5406 Å. The operating conditions are at an emission voltage of 30 kV, and an emission current of 20 mA. XRPD patterns were obtained   for crystalline phase detection between 10 and 70° (2θ).

- BET surface area

  BET surface area and pore size distribution measurements were performed using nitrogen adsorption and desorption isotherms on a Micromeritics ASAP 2000 volumetric adsorption analyzer. The $CaCO_3$ and $MgCO_3$ sorbents were degassed at 350 °C at a pressure of 10^{-6}m bar for at least 8 hr. in the degassing port of the apparatus before the actual measurements. The pore size distribution measurements were obtained using the BJH method.

- Scanning Electron Microscope (SEM)

  The morphology of the products was observed on a Hitachi S-4700 scanning electron microscope (SEM) with 15 keV of acceleration. The samples were prepared by placing the sorbents on double-sided carbon tape mounted on the sample holder.

3.4 Equipment and chemicals component

1. CO_2 analyzer (AGM4000-1-2-2) Zhi Shang instrument, Taiwan. Reaction time: T90/45, Lower Detection Limit: 1%. Sample Flow Rate: 120cc/min, Linearity Error < 2%.

2. Furnace: Thermolyne, 1400, USA

3. Magnetic stirrer: Cimares2, Thermolyne, Lowa, USA

4. Sieve: 16-30 mesh, Zhong Xin, Taiwan

5. Nitrogen (N_2) gas cylinder: 99%, Taiwan chiah lung company

6. Carbon dioxide gas cylinder: 20% CO_2/N_2, Taiwan chiah lung company

7. Air gas cylinder: Taiwan chiah lung company

8. $CaCO_3$ and $MgCO_3$:Power Research Institute , Taiwan Power Company

9. Methanol: You He company

10. Limestone: Hualien, Taiwan

3.5 Experimental apparatus TGA system

A thermo gravimetric analysis (TGA) (TG 209 F1, NETZSCH, Germany) was used to obtain the CO_2 absorbed amount.

The TGA consists of an electronic balance, vertical furnace, reactor tube, a carrier gas system, and computerized data acquisition system. The crucible is made of Al_2O_3. A schematic diagram of the TGA system for cyclic CO_2 dry absorption is shown in Figure. 3-3
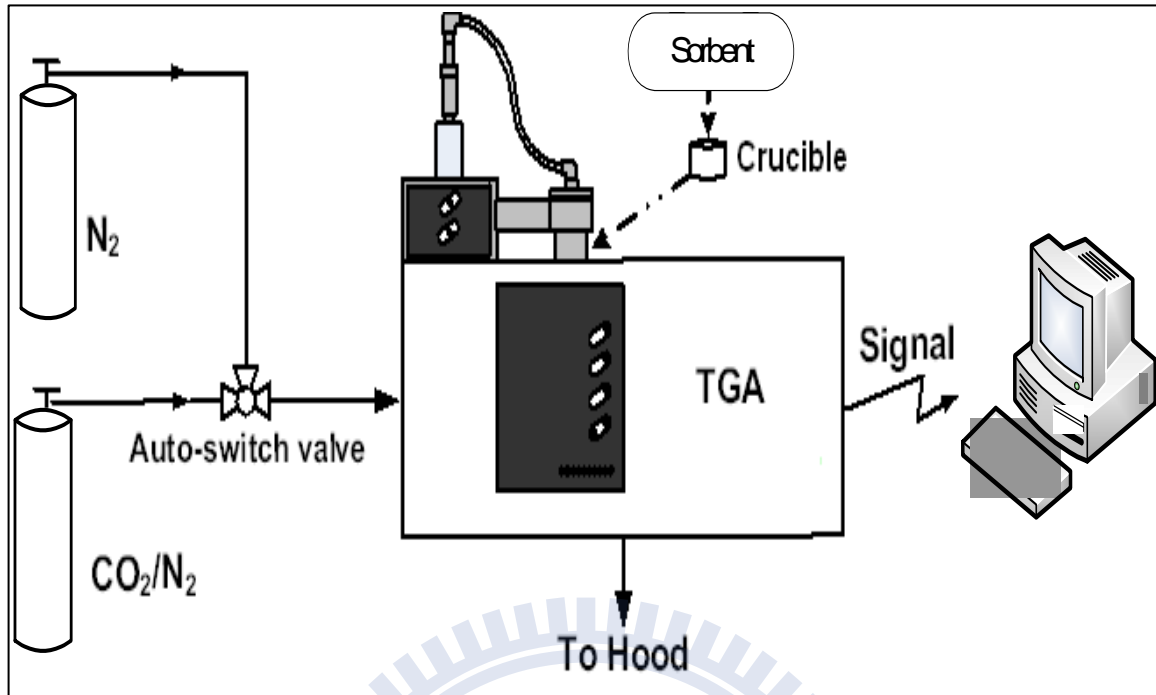
Figure 3-3 Schematic of TGA system for absorption

The two chemical reactions occurring during the cyclic test are:

$$\text{Carbonation:} \quad CaO_{(s)} + CO_{2(g)} \rightarrow CaCO_{3\,(s)}$$
$$\text{Calcination:} \quad CaCO_{3(s)} \rightarrow CaO_{(s)} + CO_{2\,(g)}$$
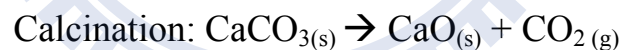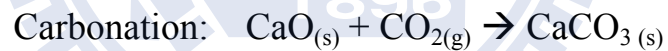
A small amount of the sample (25-30mg) was placed in the crucible; the gas flow rate was 20 ml/min for a typical run the temperature was brought at 850°C for calcination at rate of 40°C/min. After complete calcination, the temperature was decreased at a rate of 60 °C/min to the carbonation temperature. When approaching the carbonation temperature the valve was switched to allow the gas mixture of CO_2 with an inlet concentration of 20 vol% (N_2 balance) to flow over the calcined absorbent.

The conditions for TGA experiments are described in Table 3-1.

Table 3-1 Typical test condition for the cyclic test of carbon dioxide capture using TGA

Experimental parameters	Conditions
Weight of the sample	25~30 mg
Absorption cycle conditions	650-730℃, 20% CO_2/N_2, 10min
Desorption cycle conditions	850℃, pure N_2, 1min
Heating rate	40℃/min, pure N_2
Cooling rate	-60℃/min, pure N_2
Flow rate	20ccm

In order to find the optimal condition for the CO_2 capture, different parameters were also tested. Table 3-2 shows the changes in carbonation, calcination temperature, the effect of the cooling and heating rate.

Table 3-2 Change in parameters for finding the optimal conditions for the carbon dioxide capture using TGA

TGA Changes in parameters	
Effect on carbonation temperature (℃)	650, 700, 730, 760
Effect on desorption temperature (℃)	800, 825, 850
Effect of Cooling rate (℃/min)	20, 60
Effect of heating rate (℃/min)	40, 50, 60
Absorption time (min)	10, 30
Desorption time (min)	1

3.6 Packed column test system

Packed column tests were also performed to evaluate the cyclic CO_2 capture efficiency and its corresponding CO_2 absorbed amount as well. The CO_2 capture efficiency was calculated using the following equation:

CO_2 capture efficiency = 1 - C_1/ C_0,

Where C_1 is the CO_2 outlet concentration and C_0 is the CO_2 inlet concentration.

A schematic diagram of the packed column system for carbonation/calcination cyclic CO_2 is shown in Figure 3-4. For avoiding the pressure drop, all the sorbents were pelletized, crushed, and then sieved into grains using No.16 and 30 meshes (corresponding to 0.59 ~1.19 mm in grain size). 8.2±0.3g of sorbent was packed in a quartz tube with an inner diameter of 1.5 cm.
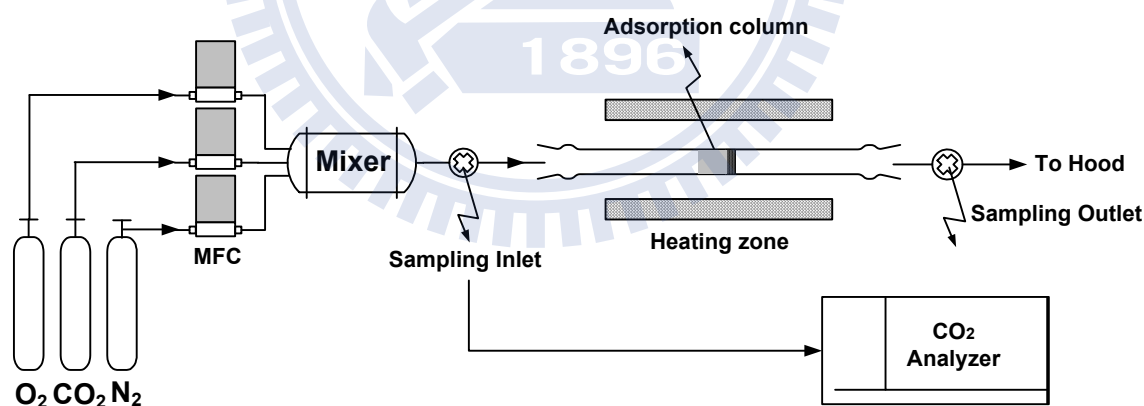
Figure 3-4 Schematic of packed column system for absorption

Before absorption, the sorbents were pretreated under N_2 flow at 850°C for 1 hour, and then the temperature was decreased to 700°C for carbonation with CO_2 inlet concentration of 15 vol. % (balanced with 6 % O_2 and 79 % N_2). The carbonation time was 10 min. After carbonation, the column temperature was increased to 850°C and kept for 30 min

under N_2 flow to release CO_2, and then the temperature was decreased to 700^oC again for the cyclic test.

The total gas flow rate was 500 ml/min (at 1 atm, 25°C) for both carbonation and calcination processes, which corresponded to an empty-bed gas residence time of around 0.36 s at absorption temperature of 700^oC. The inlet and outlet concentrations of CO_2 were continually measured by a CO_2 analyzer system (AGM$000-2000-1-2-1).

Table 3-3 shows the conditions for the packed column test

Table 3-3 Test condition for the carbon dioxide capture using packed column

Column test operation parameters	
Sorbent characteristics	(16~30 mesh 1.19 mm~0.59 mm)
Weight of the sample (g)	8.2 ± 0.3
Height (cm)	5.5
Absorption temperature (℃)	700
Desorption temperature (℃)	850
Gas mixture for absorption	15 % CO_2, 6 % O_2, 79 % N_2
Desorption Gas condition	pure N_2
Total flow rate (ccm)	500

CHAPTER FOUR RESULTS AND DISCUSSION

4.1 Characterization

The sea water precipitated $CaCO_3$ and $MgCO_3$ were characterized by XRD, SEM, and BET surface area measurements, in order to find out the chemical and physical composition, as well as the morphology of the test samples.

4.1.1 X-ray diffraction (XRD).

XRD is a non-destructive analytical technique that reveals information about the crystallographic structure, chemical composition, and physical properties of materials. Figure 4-1 shows the X-ray diffraction pattern of the $CaCO_3$, and $MgCO_3$ precipitates fresh samples and the CaO-MgO mixture sorbent after the carbonation and calcination cycle test. According to the JCPDS File No. 76-0606, the major diffraction peak of the $CaCO_3$ precipitates appears at 2θ of 29.4°. It can be observed that $CaCO_3$ is considered to be the main constituent of the calcium carbonate precipitates.

According to the index JCPDS File No. 08-0479, the major diffraction peaks of the $MgCO_3$ precipitates appear at 2θ of 30.90° and 41.92 °. As can be seen from these results, the mixed compounds of hydromagnesite $(Mg_5(CO_3)_4(OH)_2.4H_2O)$ and dypingite $(Mg_5(CO_3)_4(OH)_2 \cdot 5H_2O)$ are considered to be the potentially main constituents of the precipitated magnesium carbonates (Botha and Strydom 2001).

A similar XRD pattern for the mixture of CaO-MgO can be also observed in the study of Liu et al. (2010)
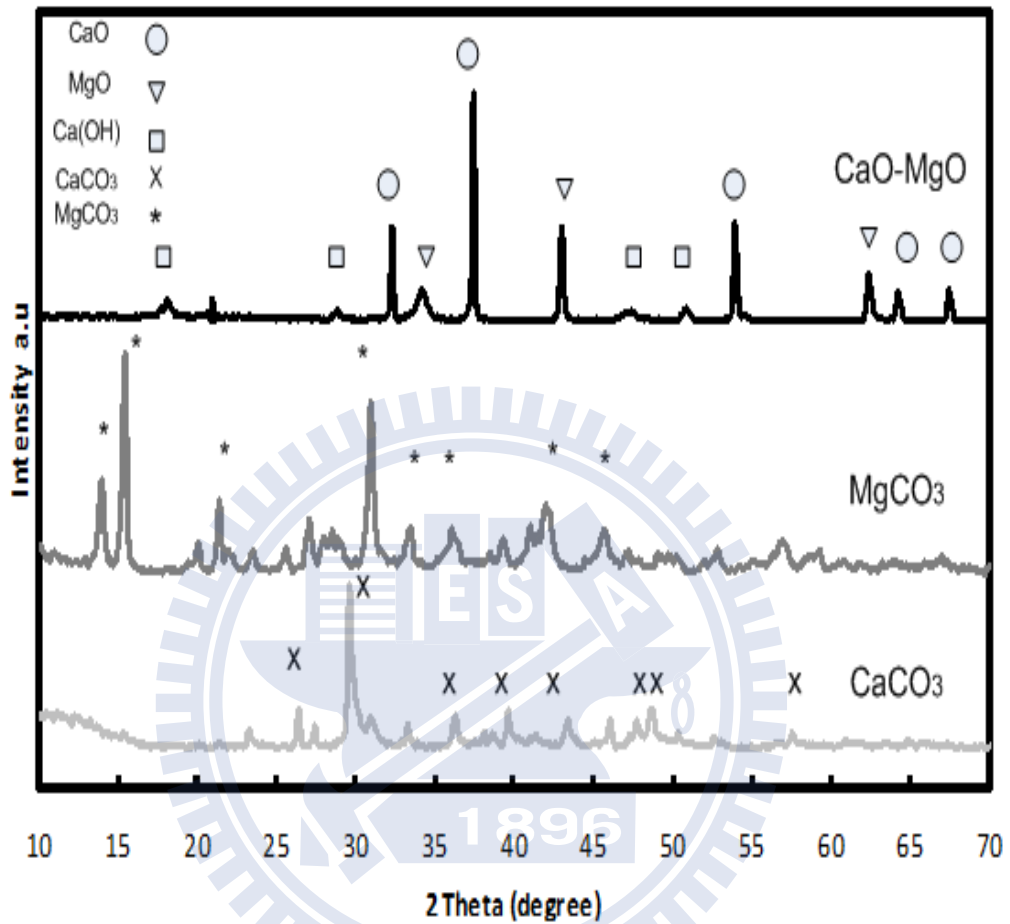
Figure 4-1 XRD of the calcium carbonate, magnesium carbonate precipitates fresh sample and CaO-MgO mixture sorbent after carbonation/calcination cycles.

4.1.2 ICP-MS analysis

Trace metallic impurities in this compound were determined using an inductively coupled plasma mass spectrometer (ICP-MS).   According to the results, 79 wt% of calcium and a 21 wt% of magnesium are present in the sample of $CaCO_3$ sea water precipitates. For the case of the $MgCO_3$ sea water precipitates the 99.5wt% of Mg and 0.45wt% of Ca are present in the $MgCO_3$. The date indicated a corresponding 55 wt % of $CaCO_3$. 21wt% $MgCO_3$ and the remaining 24% of impurities in the $CaCO_3$ precipitates sea water sample. And an almost pure sample of $MgCO_3$ sea water precipitates. Concentration of metallic impurities found in weight percent and ppm level are present in Table 4-1

Table 4-1 Concentration for metallic impurities in $CaCO_3$ and $MgCO_3$ sea water precipitates by ICP-MS

$CaCO_3$	ppm	%	$MgCO_3$	ppm	%
Na	4880.0		Na	10423	
Mg		5.88	Mg		29.07
Al	43.26		Al	164.0	
Ca		22.06	Ca		0.13
Cu	35.60		Cu	14	
Zn	171.3		Zn	86.21	
Sr	3447		Sr	24.58	
Pb	7.960		Pb	1.588	
			K	1199	
			Si	3130	

4.1.3 BET surface area analysis

One of the most important absorbent properties is the pore size and pore size distribution. Figure 4-2 (a) shows the pore size distribution curve for calcium carbonate composite treated by the precipitation process; it was found a pore size of 8.43 nm for the fresh sample. Figure 4-2(b) shows the pore size distribution curve for the Magnesium carbonate composite treated by the precipitation process, it was found a pore sized of 5.14 nm for the fresh sample. Figure 4-2(c) shows the pore size distribution curve for the CaO sorbent after, it was found a pore sized of 7.8 nm. Figure 4-2(d) shows the pore size distribution curve for the CaO-MgO mixture sorbent, it was found a pore sized of 7.6 nm for the fresh sample.

Table 4-2 shows the surface area and pore volume of the $CaCO_3$ and $MgCO_3$ fresh sample, CaO and CaO-Mixture sorbent after 10 carbonation and calcination cycle test. It can be observed that after the cycles the CaO surface are slightly decrease, and the CaO-MgO mixture sorbent the surface area is increased compare to the pure $CaCO_3$.

Table 4-2 $CaCO_3$ and $MgCO_3$ precipitates from sea water fresh sample, CaO and CaO-MgO mixture sorbent after carbonation/calcination cycles surface area and pore volume

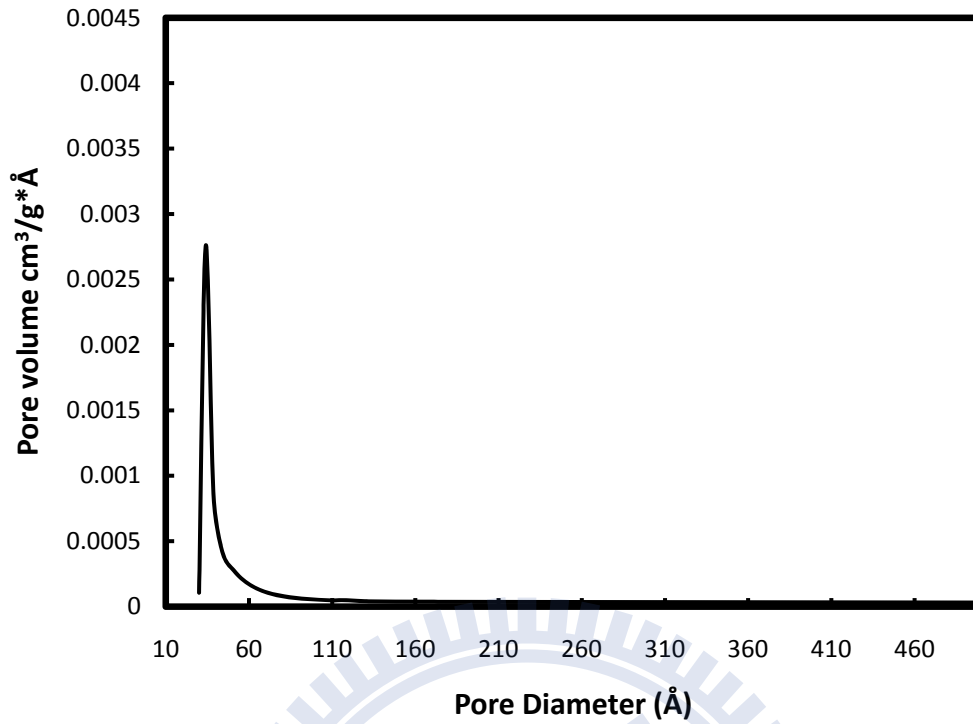| Sample	Cyclic no.	S_{BET} (m^2/g)	Vm (cm^3/g)
$CaCO_3$	fresh	17.00	0.03
$MgCO_3$	fresh	93.80	0.11
CaO	10	15.66	0.03
CaO-MgO	10	49.42	0.12

Figure 4- 2 (a) Pore size distribution CaCO₃ precipitates from sea water
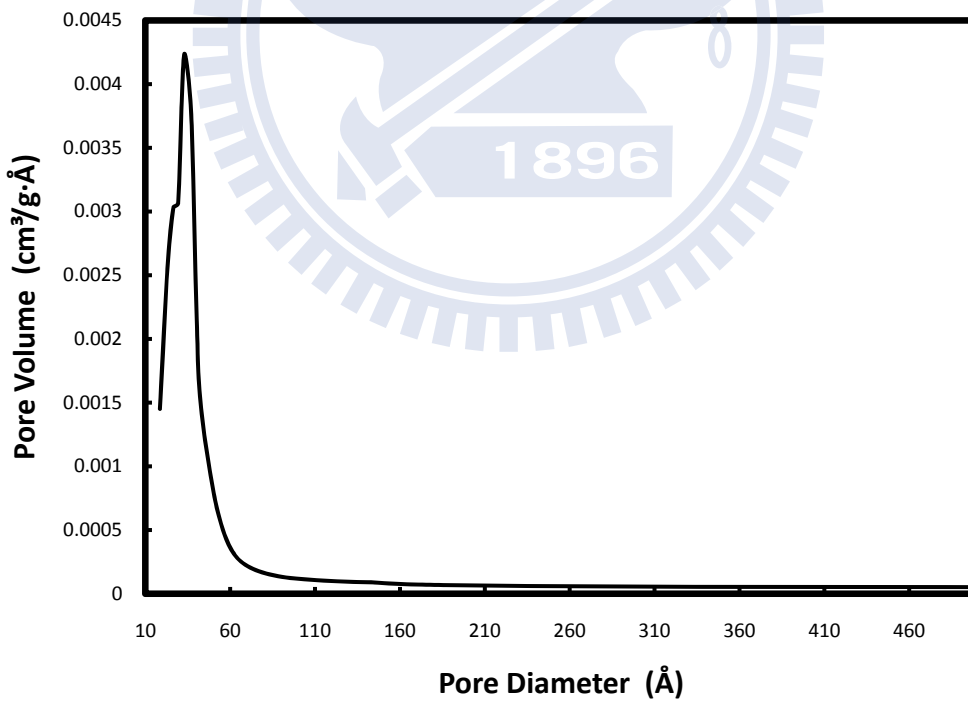

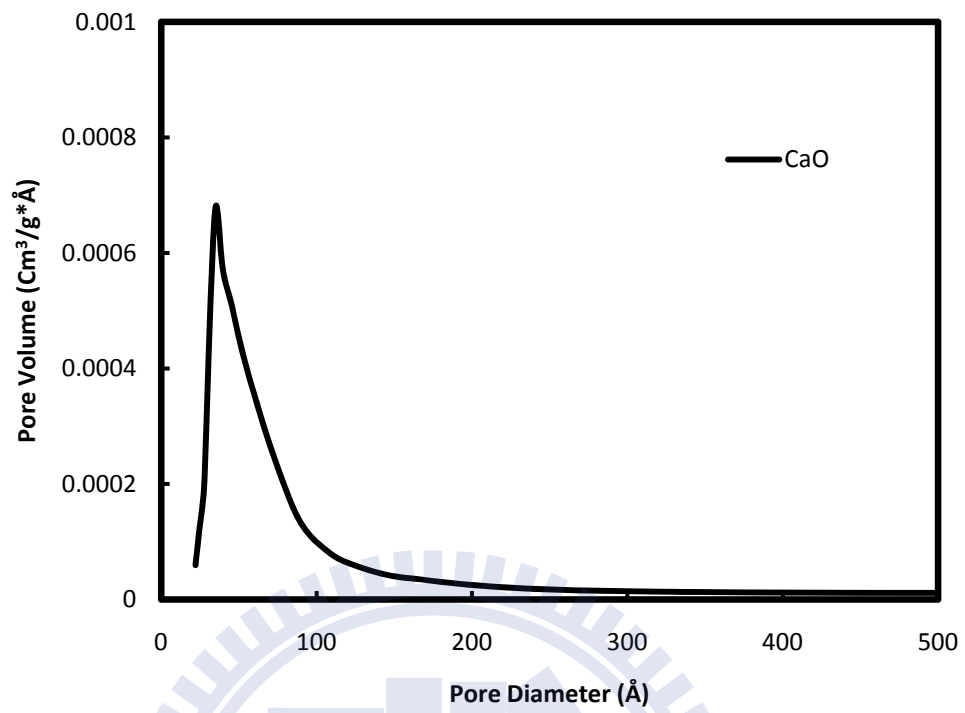**Figure 4-2 (b) Pore size distribution MgCO₃ precipitates from sea water**

Figure 4-2 (c) Pore size distribution CaO after carbonation/calcination cycles
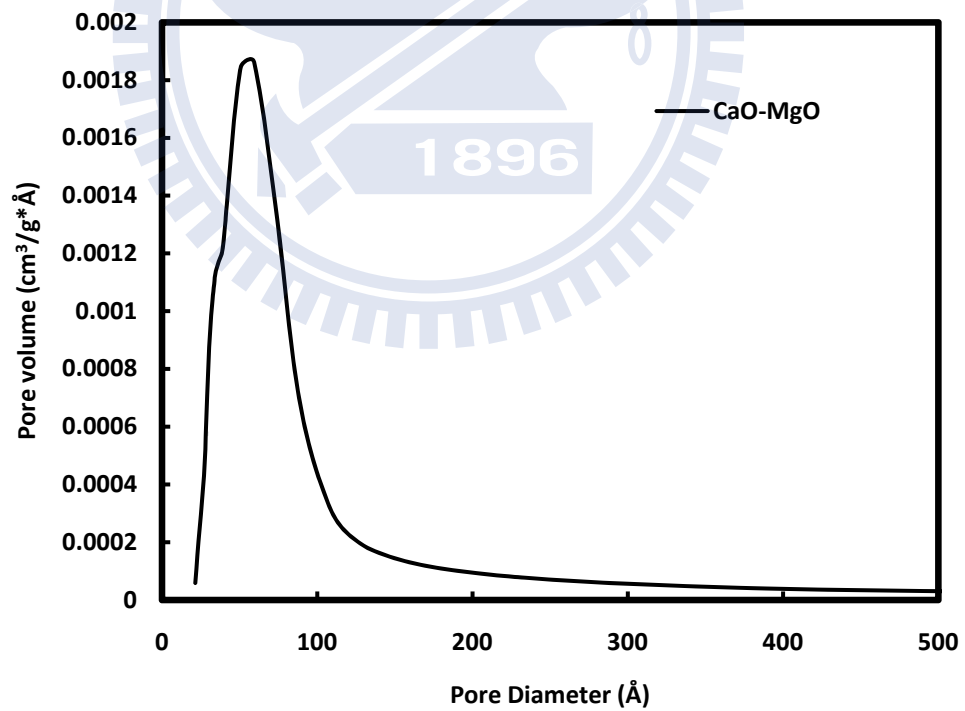
Figure 4-2 (d) Pore size distribution CaO-MgO after carbonation/calcination cycles

4.2 CO$_2$ absorption temperature range

The determination of an adequate temperature range for carbonation plays an important role in the CO$_2$ absorption process due to that the rate of reaction is sensitive to temperature. It is also of great importance to determine if an increase or decrease in temperature has an impact on the deterioration of the sorbent over repeated calcination/carbonation cycles.

4.2.1 Determination of the optimal absorption temperature

Figure 4-3(a) shows the CO$_2$ absorbed amount curve, in which the CO$_2$ was allowed to pass from 850°C to 25°C. In order to find the maximum temperature at which the reaction between the CaO and the CO$_2$ starts to occur. It can be observed from Figure 4-3(b) at 773°C the absorption process started with a very slow rate. Between 750°C and 700°C the absorption rate increases fast at rate of 0.076 (g/g-min) then between 700°C and 682°C, the reaction rate start to decrease, after 682°C the sorbent get saturated and the reaction rate is too low. Figure 4-4 (a) the absorption process was reversed by passing the CO$_2$ from 25 °C to 850 °C so the minimum required temperature for the CO$_2$ absorption can be determined. The absorption initially occurs at around 500 °C with a slow rate, it gradually increases until the highest absorption rate of 0.015 (g/g-min) was achieved at 773°C, this can be observe in Figure 4-4 (b). This is in agreement with Hughes et al. (2004) who found that temperatures below 650°C led to reaction rates too low to achieve high CO$_2$ absorption capacity. Similarly Sillaban and Harrison (2005) found a limitation in carbonation temperature bellow 778°C. Reasonable agreement was found in Symonds et al. (2009) study which indicates that at temperature below 580°C would result in extremely slow rates of

carbonation not applicable for effective CO_2 removal.
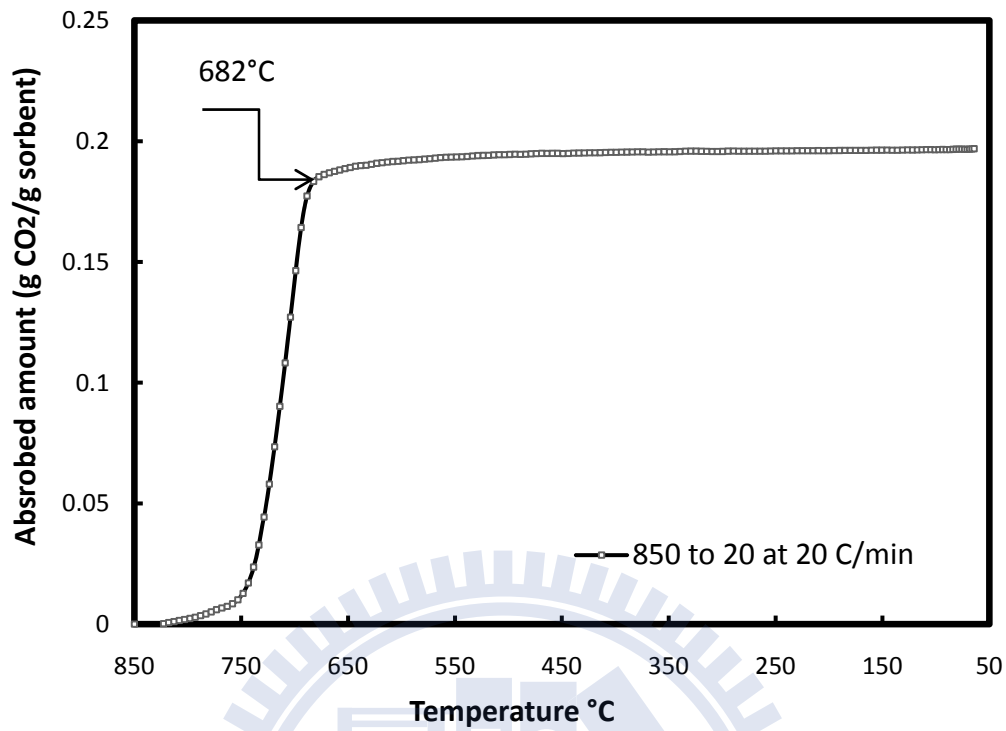
Figure 4-3 (a) CO_2 absorption curve. Decreasing temperature from 850°C to 20°C at 20°C/min
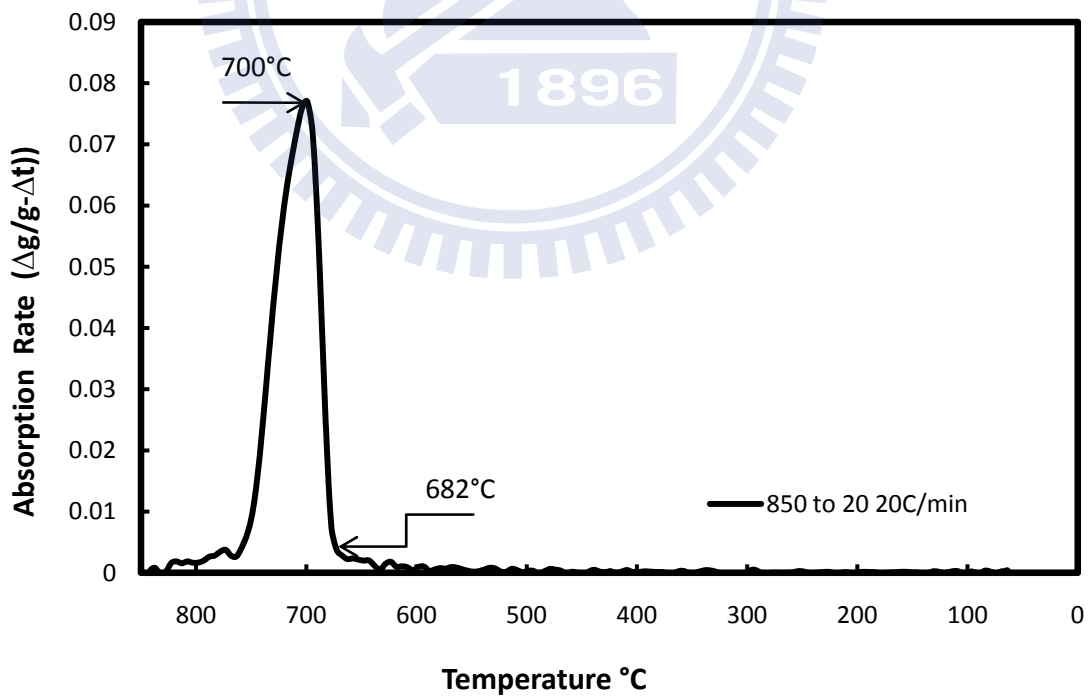
Figure 4-3 (b) CO_2 Absorption rate curve. Decreasing temperature from 850°C to 20°C at 20°C /min
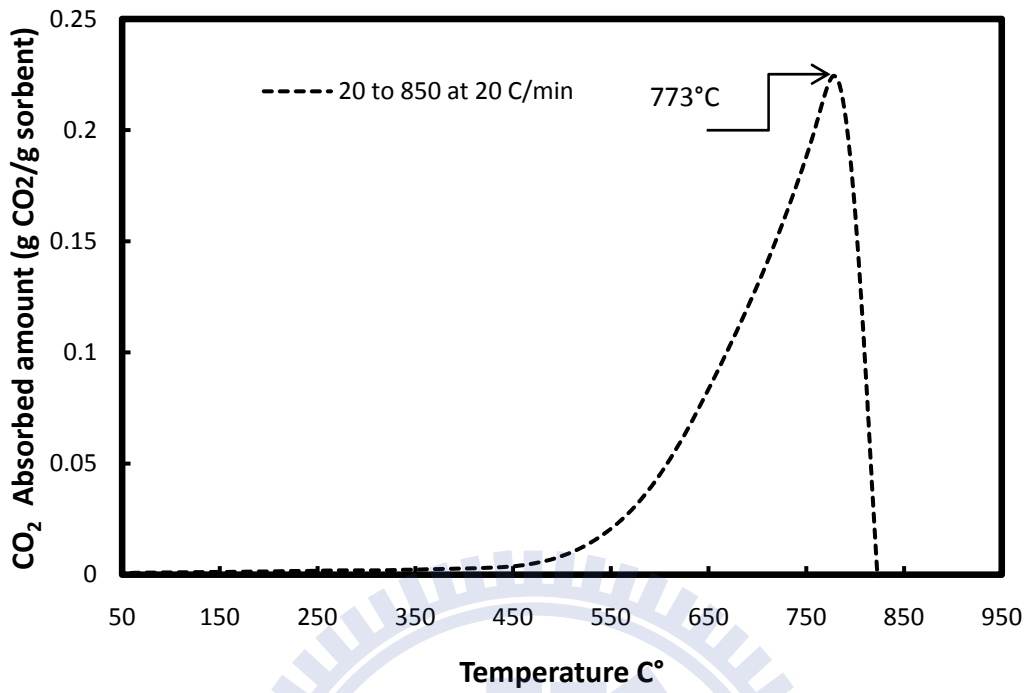
Figure 4-4 (a) CO$_2$ absorption curve. Increasing temperature from 20°C to 850°C at 20°C /min
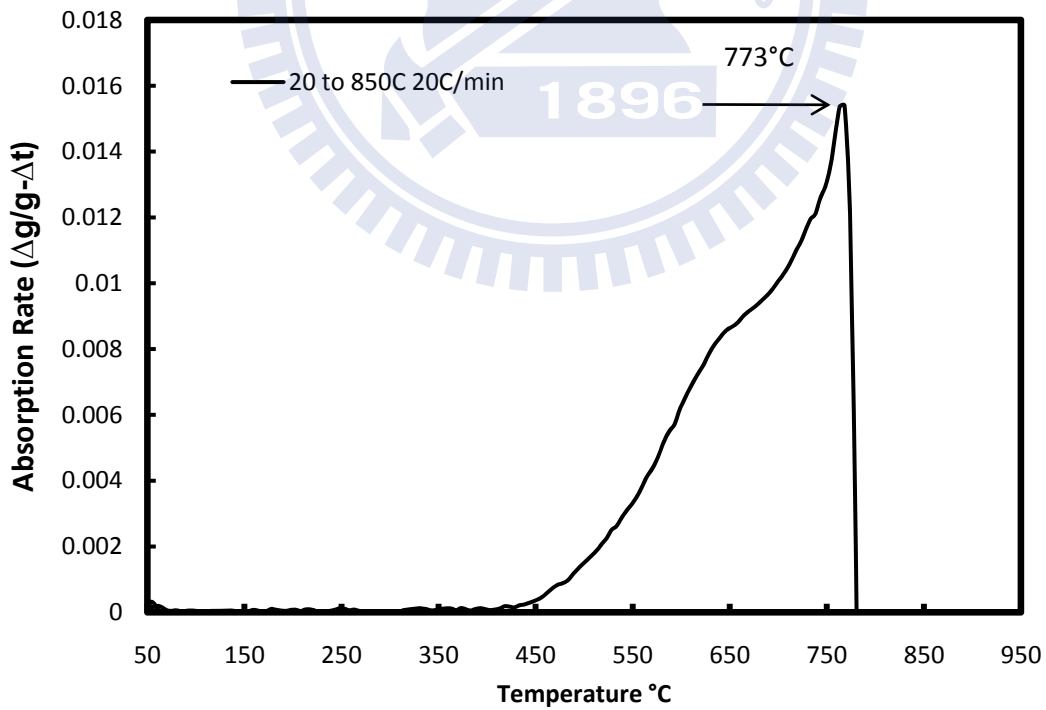
Figure 4-4 (b) CO$_2$ Absorption rate curve. Increasing temperature from 20°C to 850°C at 20°C /min

43

4.2.2 Effect of the cooling rate to determinate the optimal absorption temperature

To study the effect of cooling rate on the optimal absorption range for the CO_2 capture, the CO_2 was allowed to pass from 850 °C to room temperature; three different cooling rates were tested, at 10, 20, and 60°C /min. The results are shown in Figure 4-5(a) and Figure 4-5 (b). It is found that the optimal absorption range shift to lower temperature value as the cooling rate is increasing. It can be observed respectively at 60°C /min and 10°C /min cooling rate, the absorption rate is too low for temperature below 622°C and above 760°C, also the CO_2 absorbed amount is higher as the cooling rate is slower. Based on the minimum and maximum temperature, four temperatures were chosen for carbonation runs. These temperatures were 650°C, 700°C, 730°C and 760 °C.
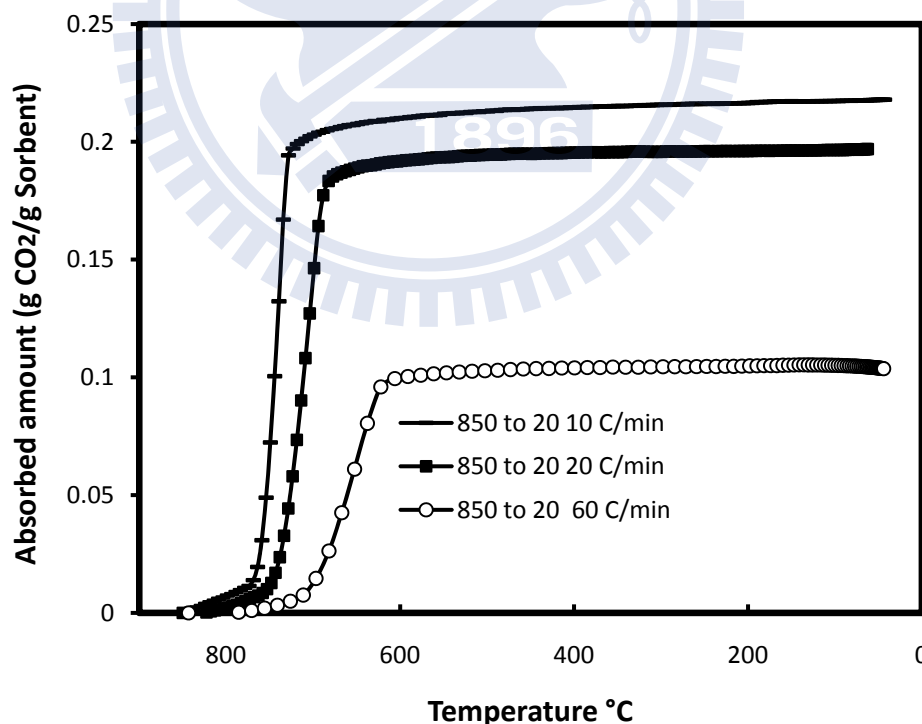
Figure 4-5 (a) CO_2 absorption curve. Effect of cooling rate at 10° C/min,   20° C/min and 60 ° C/min.
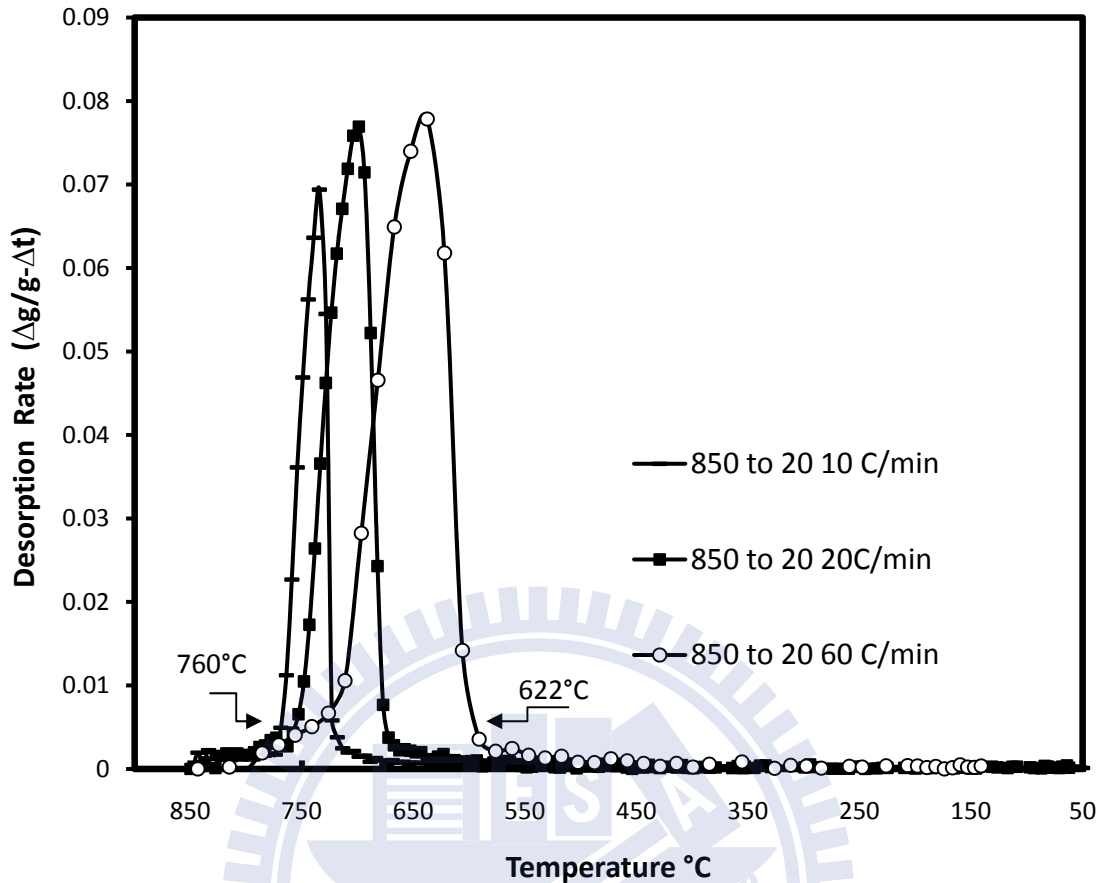
Figure 4-5 (b) Desorption rate curves at different cooling rates.

4.3 Desorption temperature

Calcination was carried out by TGA tested at three temperatures, namely 800°C, 825°C, and 850°C, and carbonation was carried out for 10 min at 700°C for 2 cycles, in order to obtain an adequate desorption temperature.

Figure 4-6 (a) shows that at 800°C the desorption rate is too low and is not complete. Addionally at temperatures 825°C and 850 °C, complete calcination was achieved in matter of minutes, with a faster desorption rate at 850°C.   In Figure 4-6 (b) it can be seen that in terms of absorbed amount both 825°C and 850°C are quite similar absorbed amount. However the desorption rate is faster at higher temperature.

Base on the previous results and other studies such as Li et al. (2006) where 850°C is considered a mild calcination temperature and higher than 950°C is considered a severe calcination, the desorption temperature of 850°C was chosen. Also in the study Grasa and Abanades (2006) has shown the effect of calcination temperature on the sorbent performance up to a maximum temperature of 1000°C. In a range of temperature up to 950°C the calcination temperatures did not affect the sorbent performance significantly and at lower calcination temperatures only a modest improvement in the results of the absorbed amount. But at 1000°C calcination temperature was a deterioration of the sorbent was observed.
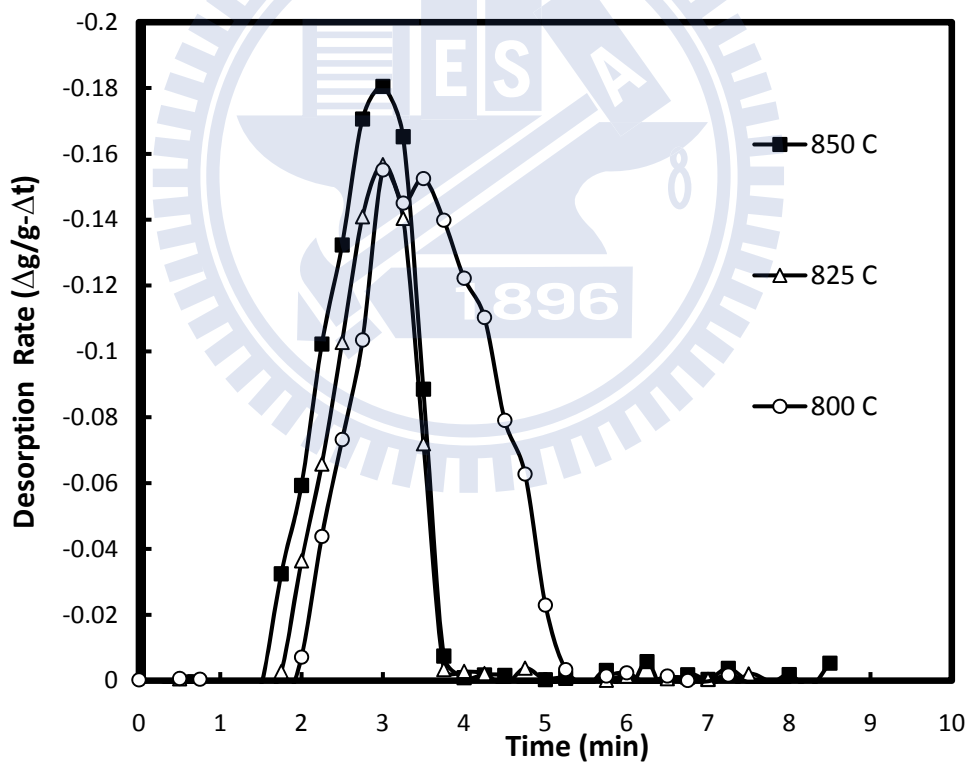
Figure 4-6 (a) CO$_2$ desorption rate. At 800°C, 825°C and 850 °C
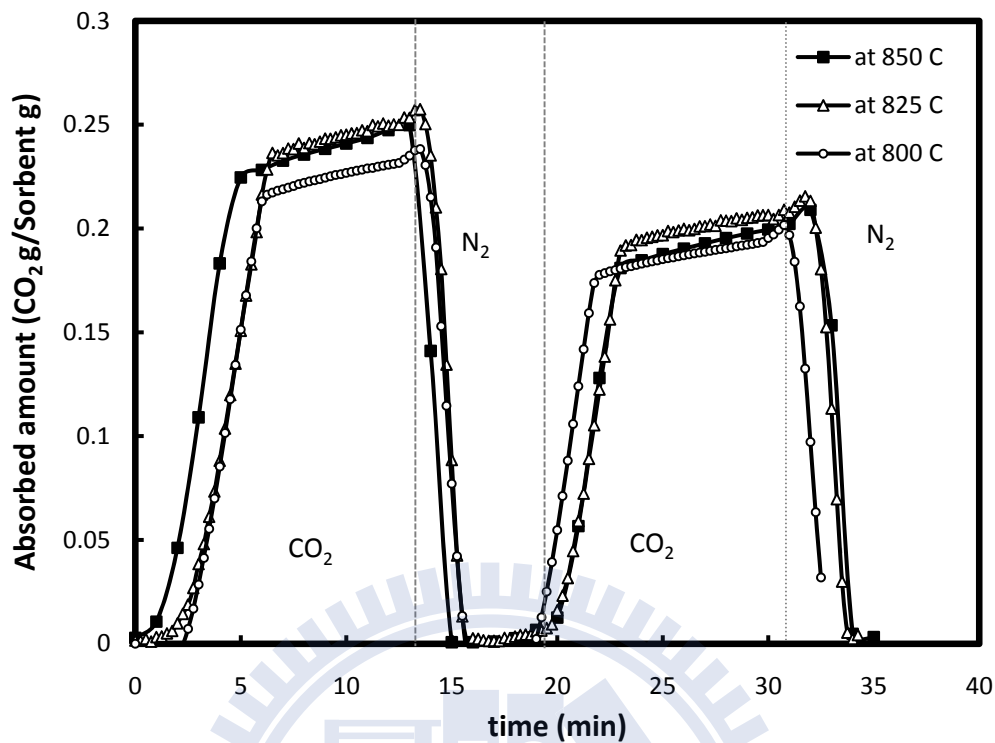
Figure 4-6 (b) CO₂ absorption curves at 800°C, 825 °C, and 850°C desorption temperatures. The carbonation temperature 700°C

4.4 CO₂ absorption at constant absorption temperatures

In order to study the effect of absorption temperature on the absorbed amount and absorption rate, four different temperatures based on the results of the absorption range for carbonation were chosen, being these 650°C, 700°C, 730°C and 760°C. The carbonation time was kept constant for 30 min and the desorption time was 10 min at 850°C. The results are shown in Figure 4-7 (a) for the absorbent amount and Figure 4-7 (b) for the absorption rate.

The carbonation temperature has a strong effect on the carbonation reactions of CaO as is mentioned by abanadez and Alvares (2003). Figure 4-7(a) shows that at a low temperature of 650°C or a high temperature of 760°C either the absorbed amount or absorption rates are not beneficial

for the absorption process compared to the absorbed amount at 700°C and 730°C. Figure 4-7 (b) shows the absorption rate that at 760 °C has the lower absorption rate, confirming that this temperature is not appropriate for the absorption process. It is also observed that at 650°C there is a higher absorption rate, but the saturation in the absorption process was reached fast, as a result the absorbed amount is lower than a 700°C and 730°C. Therefore a range from 650°C to 730 °C would be desirable for the CO_2 absorption process.

Based on these results three different cyclic tests would be performed at 650°C, 700°C, and 730 °C in order to study the behavior of the decay in the absorbed amount.
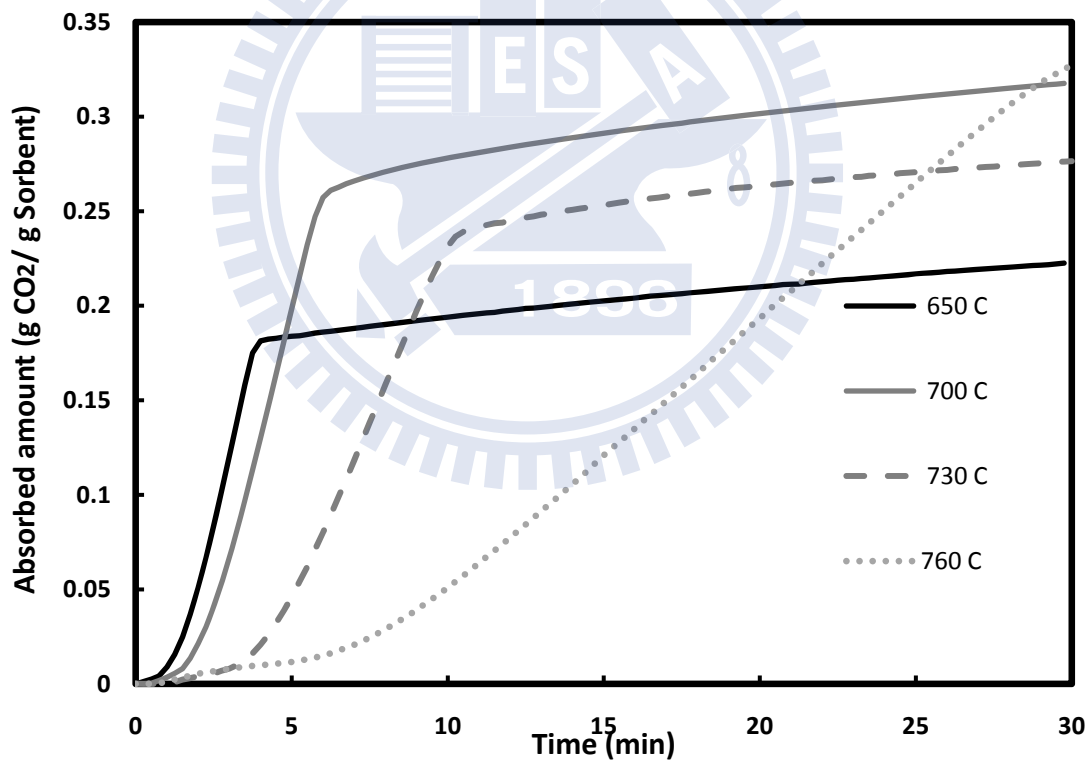
Figure 4-7 (a) CO_2 absorbed amounts at 650°C, 700°C, 730°C, and 760 °C. Desorption temperate 850°C. Absorption time 30 min
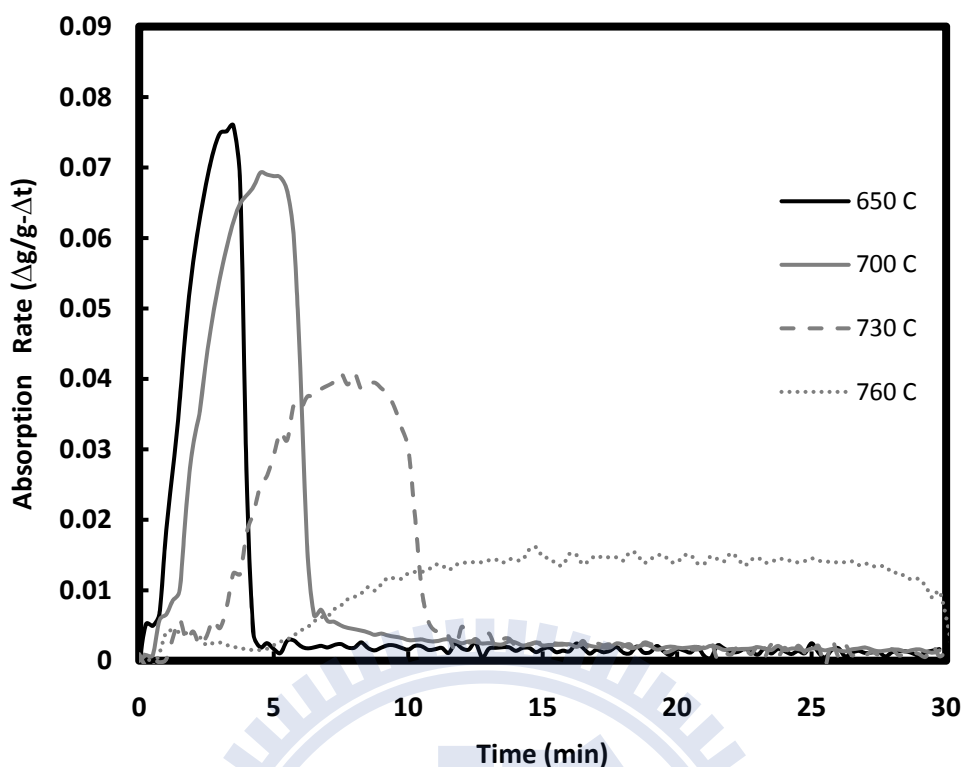
Figure 4-7 (b) CO₂ absorption rates 650°C, 700°C, 730°C, and 760 °C. Desorption temperate 850°C.

4.5 Cyclic test at different absorption temperatures

Figure 4-8 shows the cyclic test at three different temperatures. It can be seen that the absorbed amounts during the first cycle reached 174, 279, and 238 mg CO_2/g sorbent for 650°C, 700°C, 730°C respectively, and decay to about 54, 56, and 52 % by the 12th cycle. By the 23rd cycle the absorbed amounts are, 73, 101, and 104 mg/g for 650°C, 700°C, 730 °C respectively, nearly 42, 37, and 43% of the initial absorbed amount at these three temperatures.

It is well understood that the gas solid chemical reaction between CO_2 and CaO proceeds through two principal rate controlling regimes. At the beginning, the carbonation of CaO proceeds quickly by heterogeneous surface chemical reaction kinetics. However, during this initial stage a compact product layer of $CaCO_3$ is formed on the outer regions of the

CaO particles. This two stage behavior of CaO has also been a reported (Ronald 1974; Bhatia & Perlmutter 1983) and it has been attributed to the formation of the $CaCO_3$ product layer outside the CaO core which increases the diffusion resistance of CO_2 and thus reduces the reaction rate. In Figure 4-8 it can be assume that the reason for the sudden decline in capacity is attributed to the need for CO_2 to diffuse through the newly formed product layer. Liu et al. (2009) as well as Alvarez and Abanades (2005)   confirmed that as a result of sintering, the available surface area for carbonation decreases with the number of reaction cycles, leading to lower conversions corresponding to the thickness of the product layer ($CaCO_3$) on the reacting CaO surface.
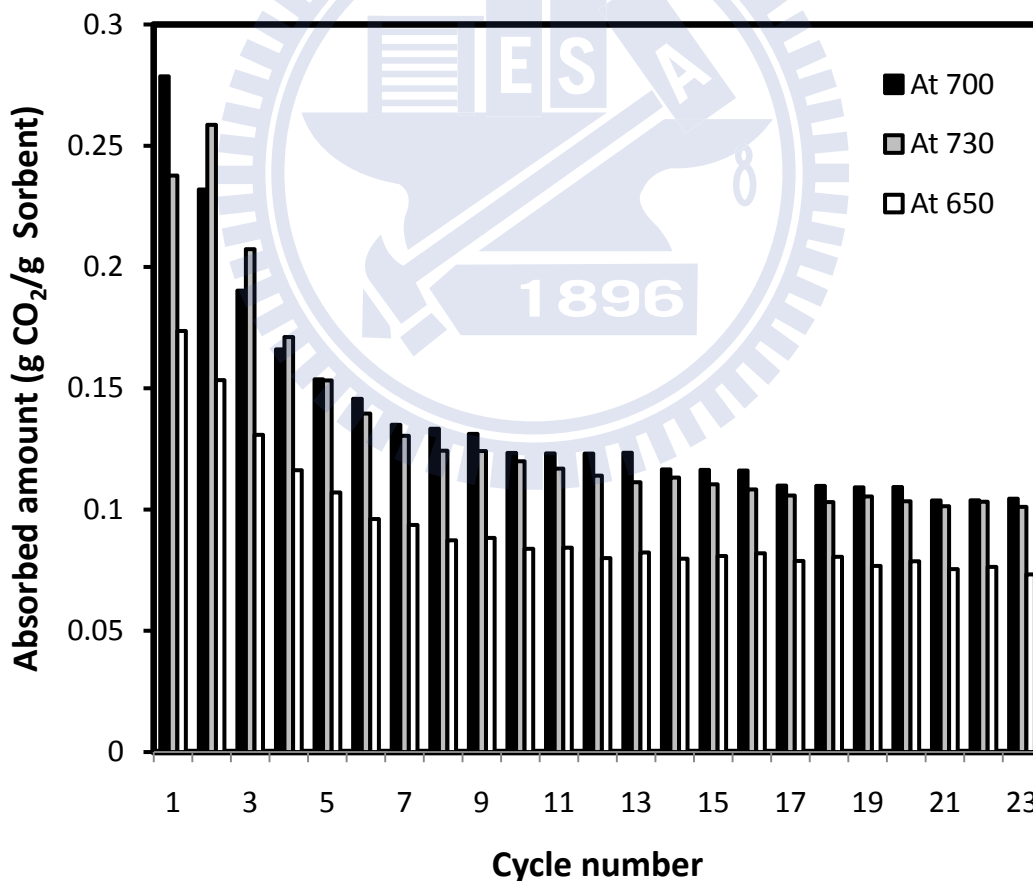
Figure 4-8 CO_2 absorption cyclic test at 650°C, 700°C, and 730°C. Carbonation time 10 min, calcination time 1 min at 850°C, heating rate 40°C /min, cooling rate 60°C /min.

4.6 Effect of heating and cooling rate

4.6.1 Effect of cooling rate on the CO_2 absorption process at 20°C/min and 60°C/min
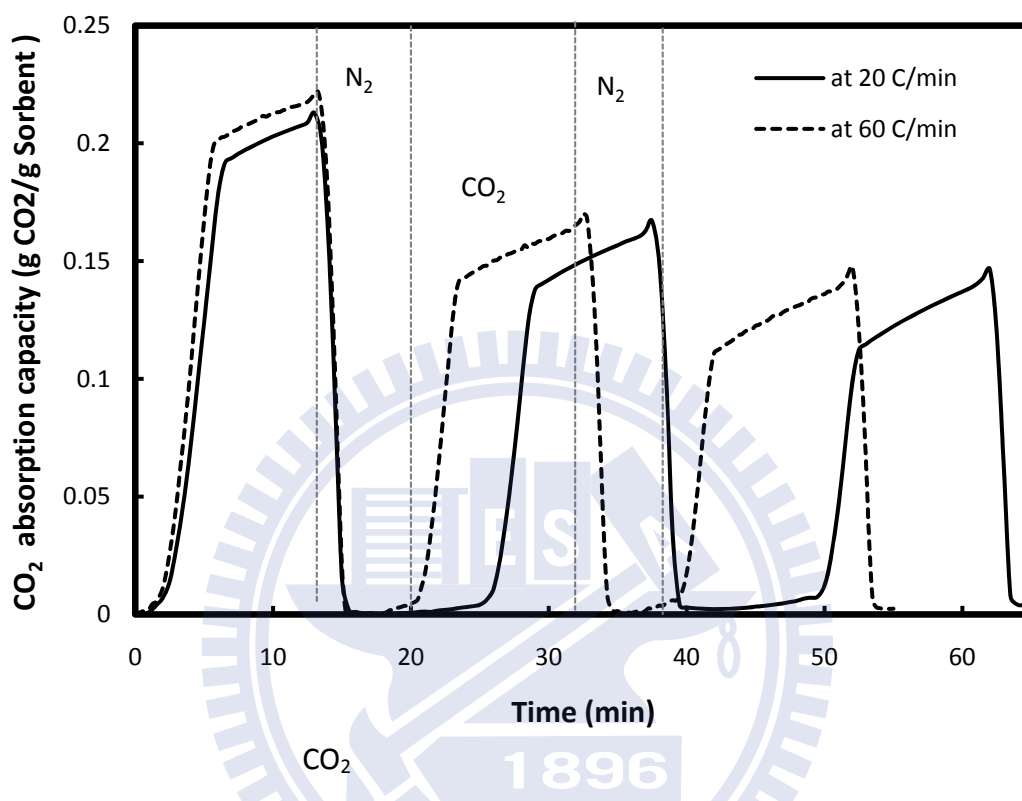
Figure 4-9 Effect of cooling rate at 20° C/min and 60 °C/min in the CO_2 cyclic absorption. Heating rate at 40°C/min, absorption time 10 min at 700°C , desorption time 1min 850°C.

Figure 4-9 shows the effect of the cooling rate over the absorption process. It can be observed that the absorbed amount at 60°C/min is slightly higher than that of 20°C /min, but the great advantage is the time saved during the process when utilize the faster rate.

4.6.2 Effect of heating rate in the CO_2 absorption process at 40 °C/min, 50 °C/min and 60° C/min

In Figure 4-10 it can be observed that the effect of the higher heating rate, which produce more sintering effect, decreasing the absorbed amount. The sintering effect present at higher heating rates is confirmed in the study of Borgwardt (1989) which found that the heating rate, rather than final temperature, was a more critical factor in terms of sorbent sintering.
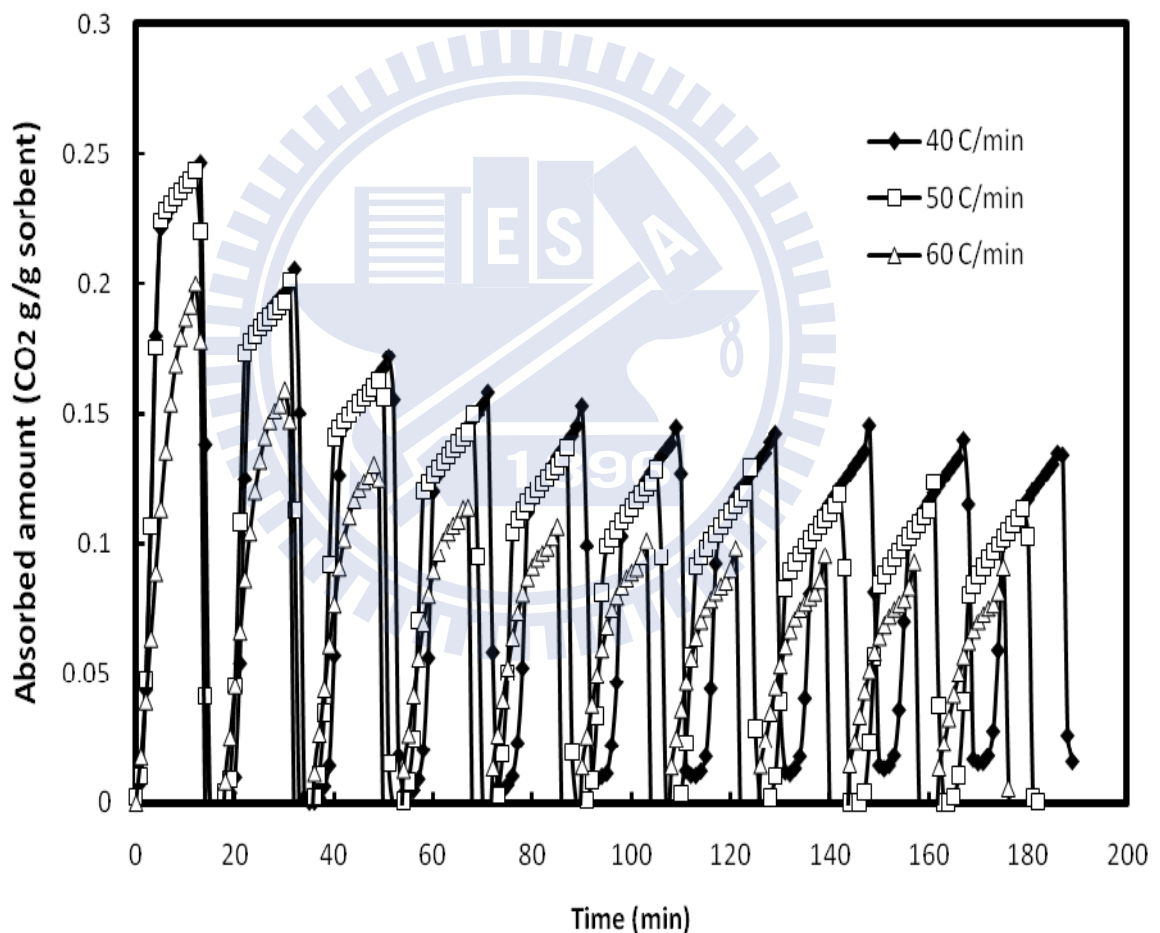
Figure 4-10 Effect of heating rate on the cyclic absorption process at 40 °C/min, 50 °C/min and 60 °C/min. Cooling rate 60°C/min, absorption temperature 700°C, desorption temperature 850°C

4.7 Effect of passing CO_2 in the cooling process.

Figure 4-11 shows the absorption curves for three cycles at 700°C during 10 min, desorption temperature 850°C for one minute, for two different conditions. With the purpose to use more efficiently the time that it takes for the desorption temperature to reach the carbonation temperature, in this case from 850 °C to 700 °C, the CO_2 was allowed to pass during this period. It is well known that the CO_2 absorption start around 770°C with a slow rate, gradually increasing until 700 °C, this condition provides an improvement in the absorbed amount. In Figure 4-11 it observed that when CO_2 was loaded at the beginning of cooling process the absorbed amount increases compared to the normal process.
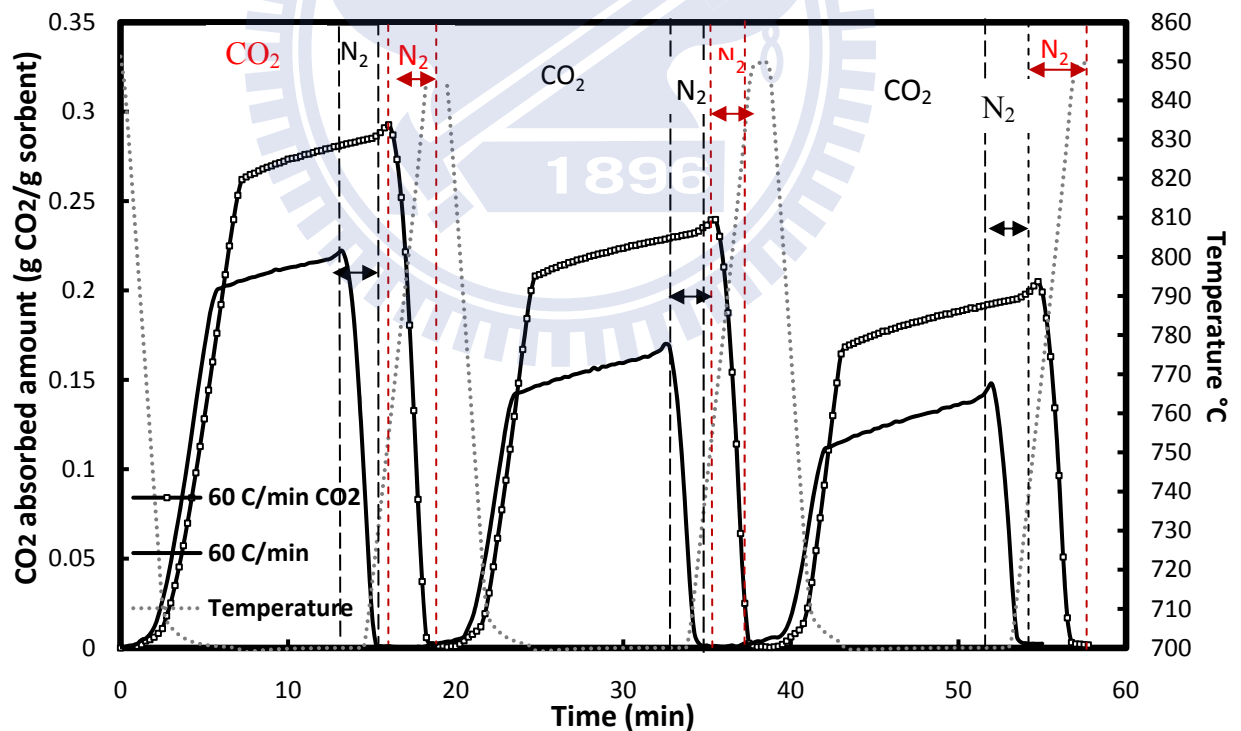
Figure 4-11 Effect of passing CO_2 in the cooling process from 850 to 700 °C for absorption. Desorption 1 min at 850°C. Heating rate 40°C/min, cooling rate 60°C/min

4.8   Mixture of $CaCO_3$ (95%) and $MgCO_3$ (5%)

One of the objectives of this work was to find a method for the production of CaO-based sorbents that could be able to prevent the sintering effect, which causes the CO_2 capture capacity of the material to deteriorate rapidly after a few cycles of utilization. Here we show a mechanical mixing method which consists of the mixture of $CaCO_3$ (95%) and $MgCO_3$ (5%) precipitates from sea water. The purpose of adding $MgCO_3$ to the $CaCO_3$ was to improve the stability of the sorbent by inhibiting sintering. This enhancement could be due the melting point of the MgO which is higher than that of the CaO and acts as a physical barrier to prevent sintering and agglomeration as is suggested in the study of Fang et al. (2009). Liu et al. (2010) also suggested that the sintering resistant nature of the sorbent is believe to be owing to the inert support material effectively separating the CaO particles.
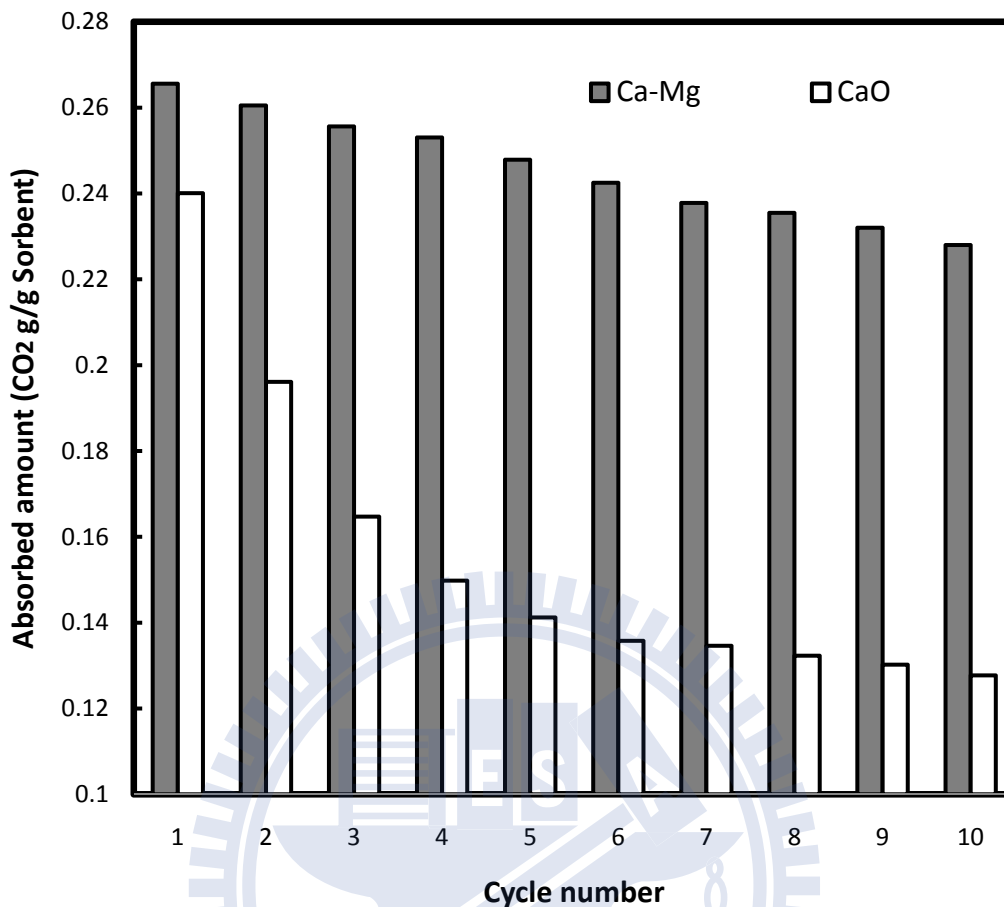
Figure 4-12 CO$_2$ cyclic absorption test for Ca-Mg mixture and pure CaO sorbent. Absorption time 10 min at 700 °C, calcination time 1 min at 850°C, heating rate 40°C/min, cooling rate 60°C/min

Figure 4-12 shows the result of the cyclic absorption test using TGA system with a fixed carbonation temperature of 700°C for 10 min, desorption temperature for 1 min at 850°C heating rate of 40°C/min and cooling rate of 60°C/min. It can be seen that the absorbed amount and stability are higher for the CaO-MgO mixture sorbent precipitates compared with the pure CaO precipitates. The absorbed amount increased in a 10%, compared to the pure CaO precipitates from sea water and decayed to 85 % after 10 cycles.

The MgO which does not absorb CO_2 under the same condition as that of CaO has a structure stabilizing effect, as can be seen in the $MgCO_3$ which present higher cycle stability compare to CaO is show in Crhissafis et al. (2009b). Li et al. (2009) also found that adding an inert material has a critical effect on the long term stability of the CaO-based absorbent. Chrissafis (2005a) indicated that mixing high melting point compounds such Al_2O_3 or MgO can avoid the effect of sintering. In Albrecht et al. (2008a) a mixture of 20%wt of MgO was produced, showing an improvement in the absorbed amount of 45% greater capacity than the original material. Without the MgO the absorbed amount was very small after several cycles.
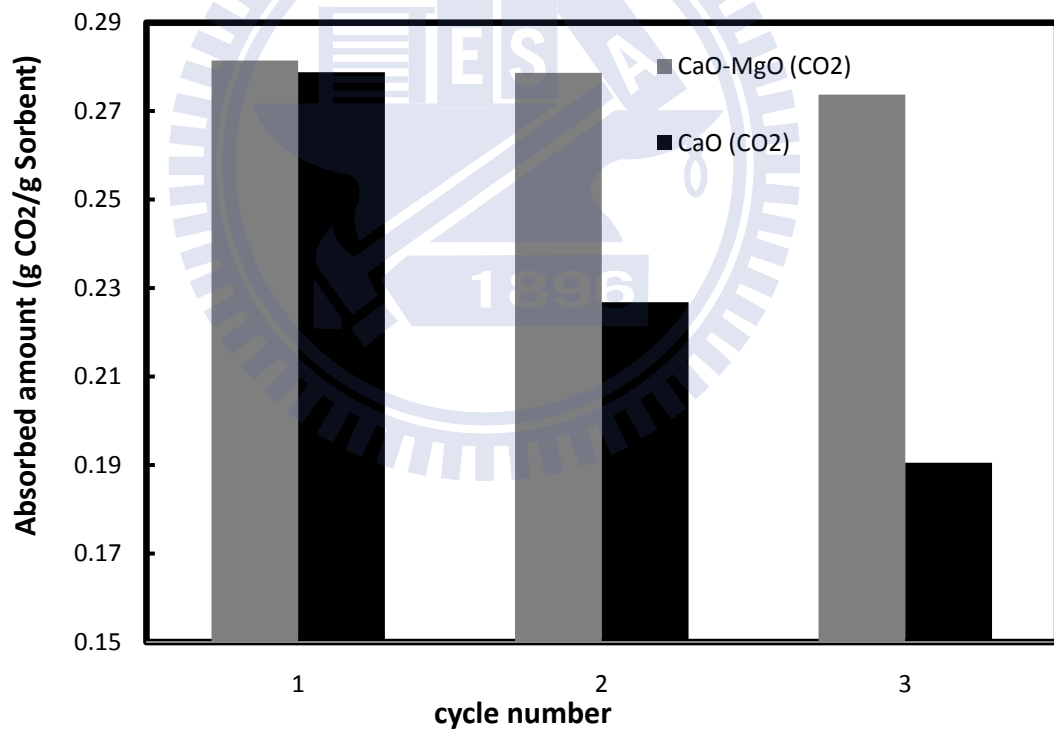
Figure 4-13 CO_2 cyclic absorption test for CaO-MgO mixture and pure CaO sorbent. Passing CO_2 during the cooling time, absorption time 10 min at 700 °C, calcination time 1 min at 850°C, heating rate 40°C/min, cooling rate 60°C/min.

56

Figure 4-13 shows a cyclic absorption test of CaO-MgO mixture sorbent and the pure CaO at 700°C for 10 min, desorption temperature 850°C for 1 min, at heating rate 40°C/min, cooling rate 60 °C/min. During this process for both of the sorbent the CO_2 was allowed to flow thought the cooling time. It can be observed that at this condition provided a better stability compared to the normal process.
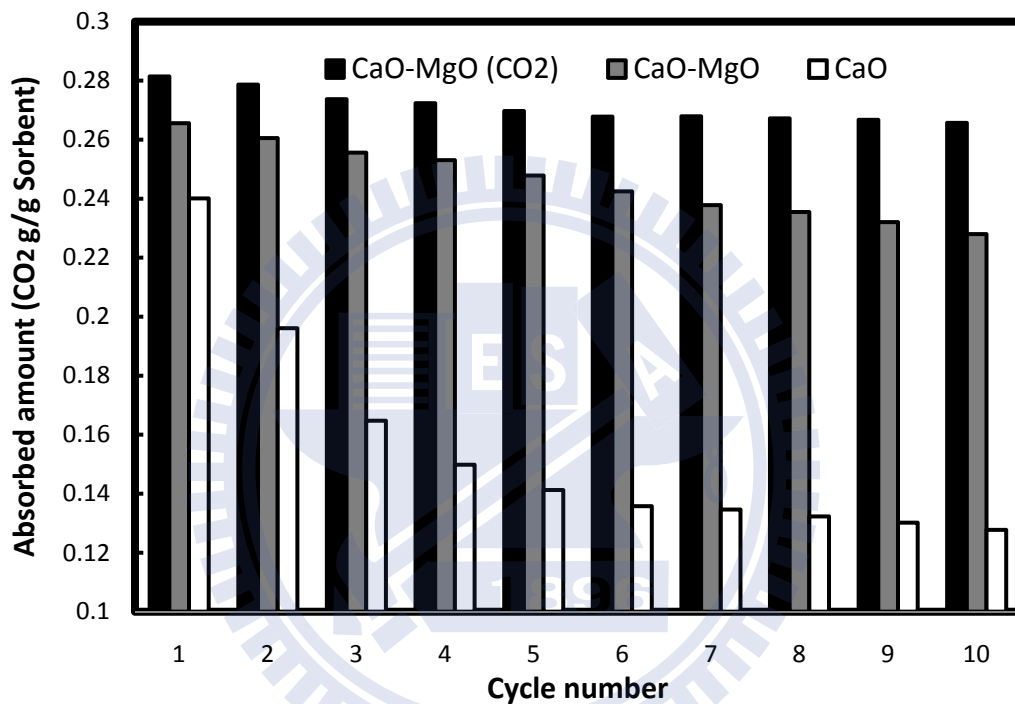
Figure 4-14 (a) cyclic absorption test for CaO-MgO mixture sorbent with and without passing CO_2 in the cooling time and pure CaO. Carbonation time 10 min at 700°C, calcination time 1 min at 850°C at heating rate of 40°C/min and cooling rate of 60°C/min

Figure 4-14 (a) shows the result of the pure CaO and the CaO-MgO mixture sorbent with and without passing CO_2 at 700°C for 10 min, desorption temperature 850°C for 1 min, at heating rate 40°C/min, cooling rate 60 °C/min. It can be observed that in the case of CaO-MgO mixture without passing CO_2 during the cooling time, the absorbed amount increased in a 10%, compared to the pure $CaCO_3$ and decayed to

85 % after 10 cycles. When passing CO_2 during the cooling time the absorbed amount increased 17%, and decayed 94 % after 10 cycles. Using the pure $CaCO_3$, the absorbed amount decays in 53% after 10 cycles. It is shown in these results that passing CO_2 in the cooling time the stability of the sorbent is more stable along the cycles, and also the method of MgO introduction plays an important role in producing stable absorbents.
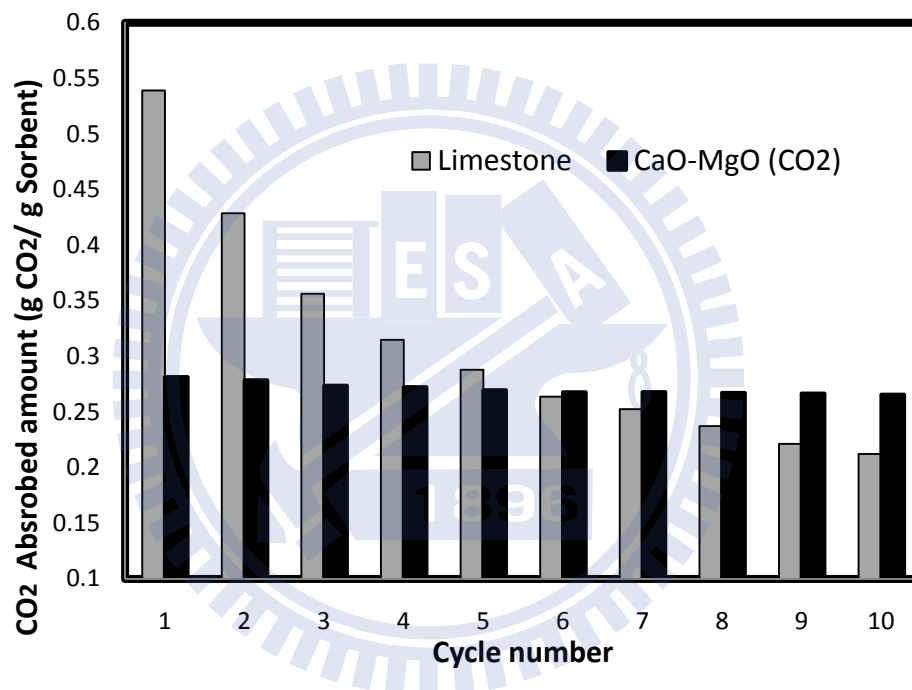
Figure 4-14 (b) cyclic absorption test for CaO-MgO mixture sorbent passing CO_2 in the cooling time and pure chemical limestone. Carbonation time 10 min at 700°C, calcination time 1 min at 850°C, heating rate of 40°C/min and cooling rate of 60°C/min

Figure 4-14 (b) shows the result of the absorption process for the pure chemical Limestone and the CaO-MgO mixture sorbent, with a fixed carbonation temperature of 700°C and a cooling rate of 60°C /min. It can be seen that the performance of the Limestone has a higher initial absorbed amount (0.53 CO_2g/g sorbent) compare to the CaO-MgO mixture sorbent (0.28 CO_2g/g sorbent) for the first cycle, but the

deterioration of the pure Limestone sorbent is more remarkable than the mixture sorbent. For the 6th cycle the absorbed amount of both sorbent are almost similar (0.26 g/g) and for the end of the last cycle the absorbed amount of the limestones was 40% of the original capacity, and the mixture sorbent the absorbed amount was 94% of the original capacity.

Figure 4-15 shows the result of the absorption process with a fixed carbonation temperature of 700°C and a cooling rate of 60°C /min, varying the heating rate at 60°C /min and 40°C /min, with a special condition in which the CO_2 was allowed to flow throughout the cooling time region. First an improvement is observed at heating rate of 40°C/min, for the stability and absorbed amount of the mixture sorbent. But as comparing the two different heating rates, it can be seen that higher heating rate of 60°C/min has more severe effect in terms of sorbent sintering, similar to what was observed by Borgwardt et al. (1989). Thus the CO_2 absorbed amount continuously decreased.
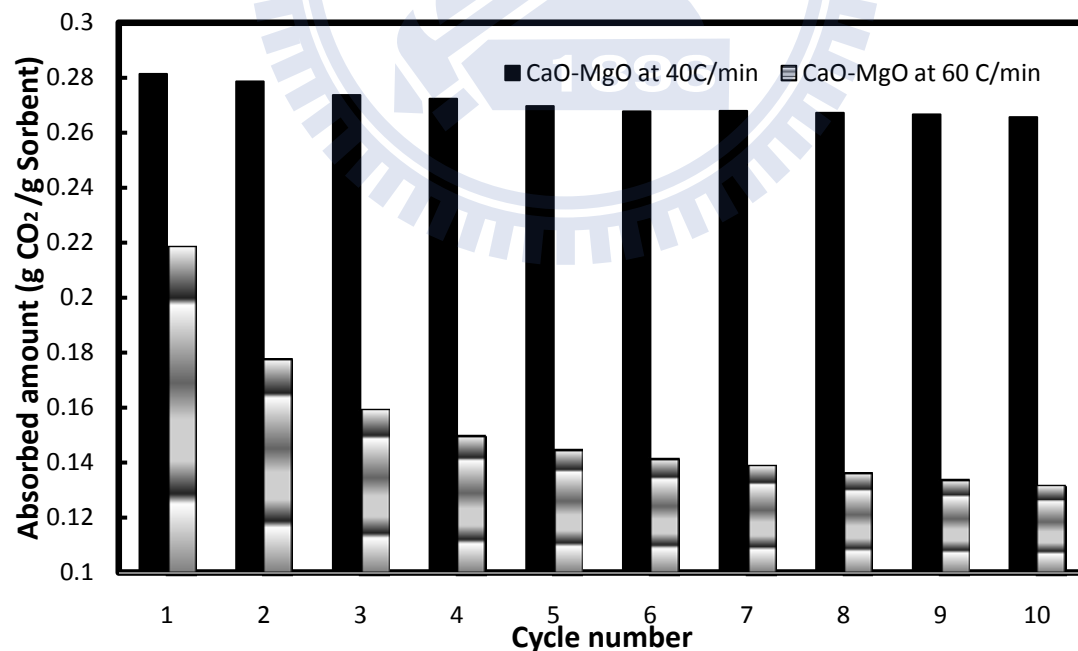
Figure 4-15   CaO-MgO mixture sorbent absorbed amount at heating rate of 40 °C/min and 60°C /min passing CO₂ in the cooling time. Carbonation temperature 700°C, calcination temperature 850°C

59

4.9 SEM images CaCO$_3$ after CO$_2$ 23 cycles at different temperatures

Figure 4-16 (a) shows the SEM image of the fresh sea water precipitates CaCO$_3$ sample. It is observed that the grain structure of the parent CaCO$_3$ fresh sample has three particle phases, a quasi spherical shape, a slides shape and square shapes.

Figure 4-16 (b) shows the carbonation effect at 650°C after 23 cycles, in which the sample suffer some sintering effect compared to the fresh one. At 650°C a poor CO$_2$ capture performance was observed. Figure 4-16 (c) and (d) gives the SEM images from 700°C and 730°C after 23 cycles, both samples presented also the sintering effect, a growth in the particles is observed being this more remarkable at 730°C. A inter granular cracking along the grain boundaries in the carbonated samples can also be observed. However, at these temperatures the absorbed amount is higher than 650°C. Base on this a temperature of 700°C is consider to be a optimal having a good absorbed amount and avoiding the more sintering effect.

Figure 4-17 shows the EDX analysis of the CaCO$_3$ fresh sample it was detected different distribution of the elements in the CaCO$_3$.
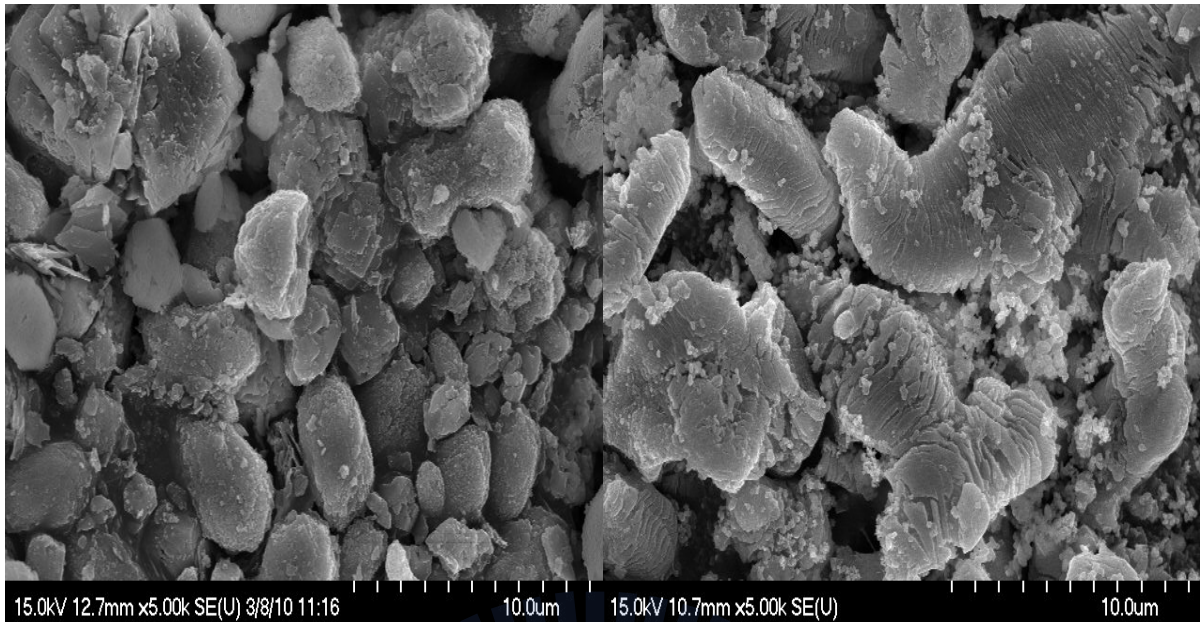
a) Fresh sample   b) After 23 cycles at 650°C
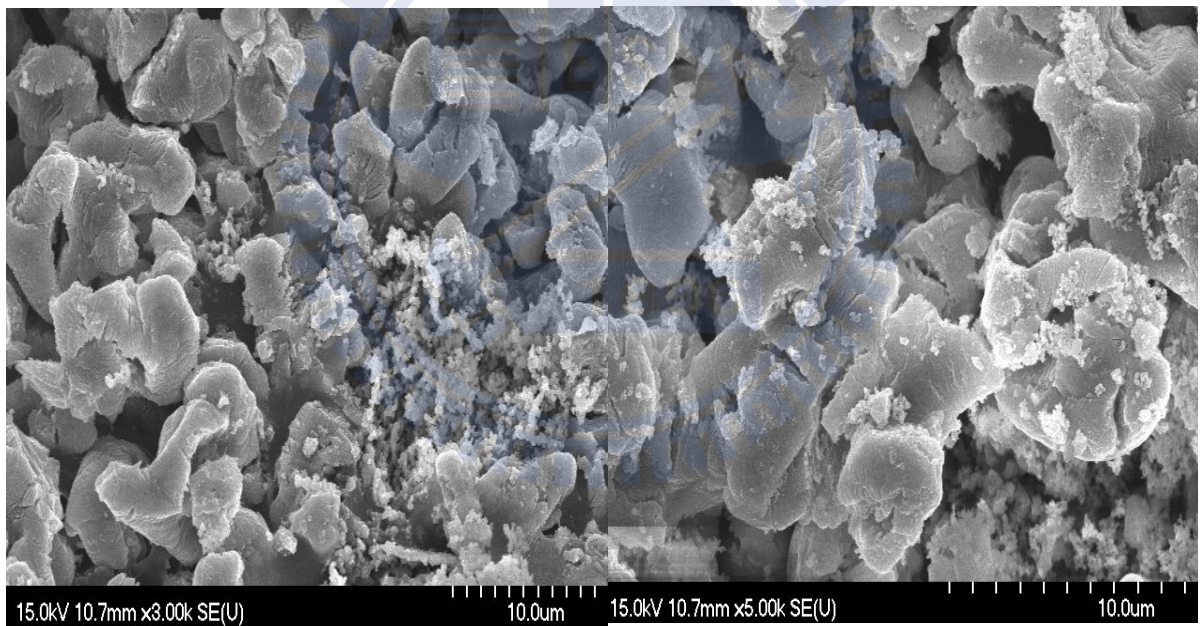
c) After 23 cycles at 700 °C   d) After 23 cycles at 730 °C

Figure 4-16 SEM images CaCO₃ precipitates from se water. a) Fresh sample b) 650°C c) 700°C d) 730°C. After 23 cycles.
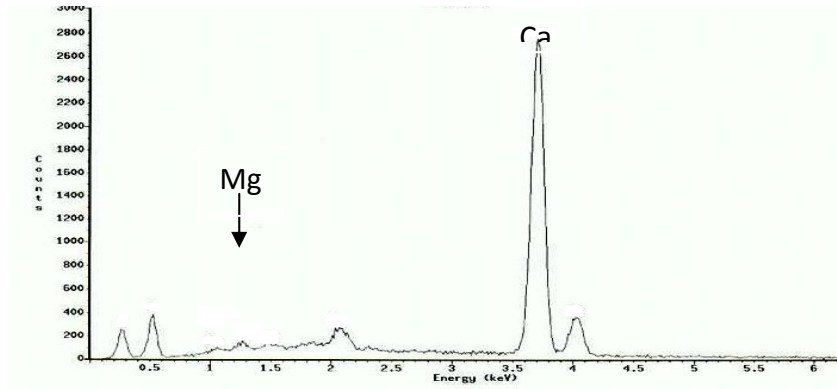
a)   Square shape
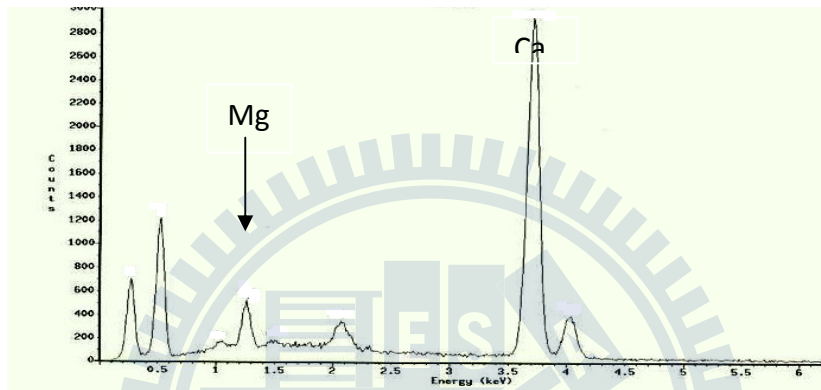
b)   Slides shape
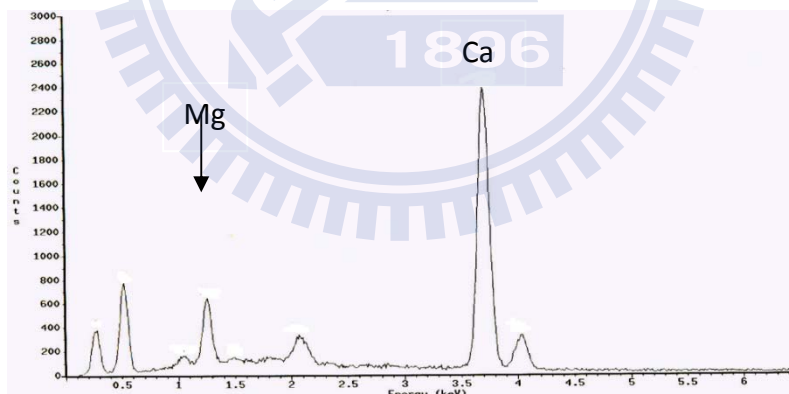
c)   Particle shape

Figure 4-17 EDX diagram of CaCO₃ precipitates from se water fresh sample. a) square shape b) slide shape c) Particle shaped

4.10   SEM images Mg-Ca mixture after CO$_2$ after carbonation/calcination cycles at 700°C using TGA

Figure 4-18 (a) shows SEM images of the fresh CaO-MgO mixture sorbent. Figure 4-18 (b) shows the sample CaO-MgO mixture sorbent after 10 cycles. In which the MgO particles are adhered in the surface of the CaO, also confirm by the Energy-dispersive X-ray spectroscopy (EDX). Because of this, an improvement in the absorbed amount was observed in the mixture sorbent compared to the pure one, both after 10 cycles.   A certain level of heterogeneous mixing appears to have benefit, probably as a result of providing stable segregation of small CaO particles (Li et al. 2009).
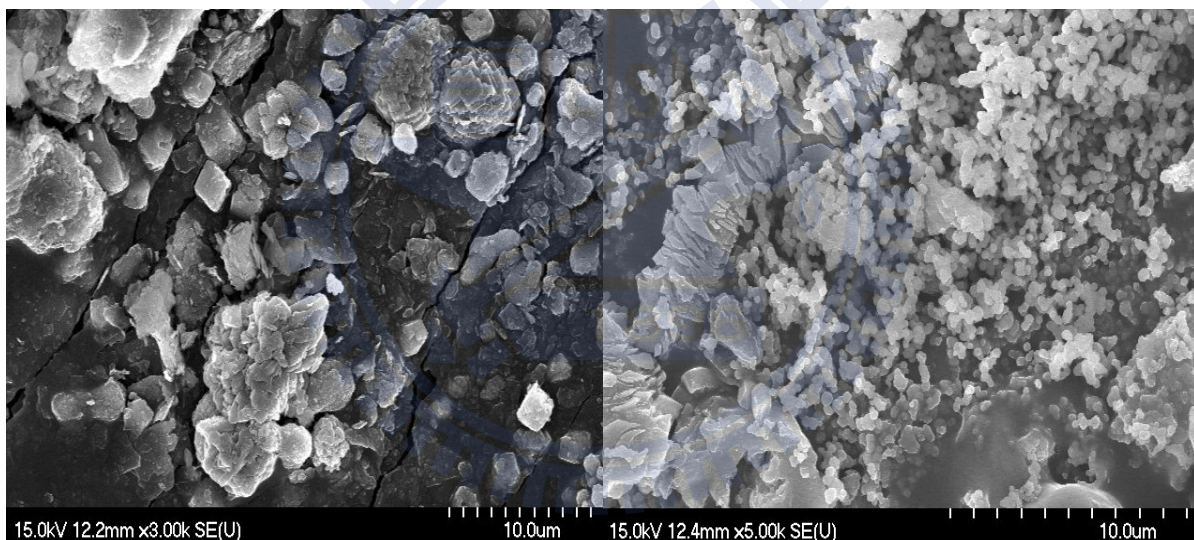
15.0kV 12.2mm x3.00k SE(U) 10.0um	15.0kV 12.4mm x5.00k SE(U) 10.0um
a) CaO sample	b) CaO-MgO mixture sorbent

Figure 4-18 (a) fresh CaO-MgO mixture sorbent (b) SEM images CaO-MgO mixture after 10 cycles . Both at 700°C using TGA at heating rate 40k/min and cooling rate 60k/min

Figure 4-19 shows the SEM images of CaO-MgO mixture sorbent at 700°C. Figure 4.-19 (a) at heating rate of 40°C/min. (b) at heating rate of 60°C/min. It can be observed that the sample with a heating rate of 40°C/min present less sintering effect than at 60°C/min, where there is more agglomeration of the particles, affecting the absorbed amount along the carbonation/calcination cyclic test. As a result of the higher heating rate, poor absorbed amount was observed.

a) Heating rate of 40°C/min   b) Heating rate of 60°C/min
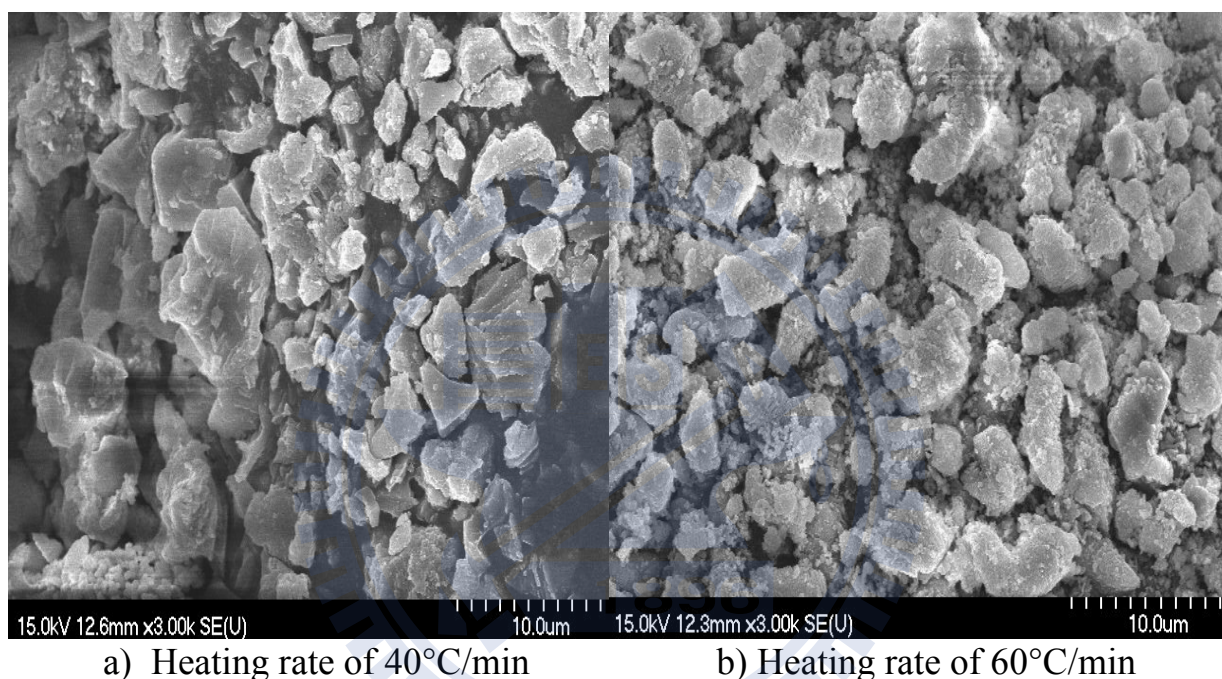
Figure 4-19 SEM images Mg-Ca Mixture at 700°C after 10 cycles using TGA. (a) At heating rate 40°C /min. (b) At heating rate 60°C /min. Both samples with a fixed cooling rate of 60°C/min passing CO$_2$

4.11 Packed column absorption test

The CO$_2$ absorbed amount of the MgO-CaO mixture sorbent and original CaO sorbent during cyclic absorption are shown in Figure 4-20. It can be seen from Figure 4-20 that the MgO-CaO mixture sorbent showed higher CO$_2$ capture efficiencies than that of original CaO sorbent.

This phenomenon is similar to that in TGA system, confirming that the MgO acted as an anti sintering sorbent. Figure 4-21 shows the CO_2 removal efficiency of the cyclic column test, it can be seen that the CaO-MgO mixture sorbent have a better removal efficiency than the pure sample after the last cycle.
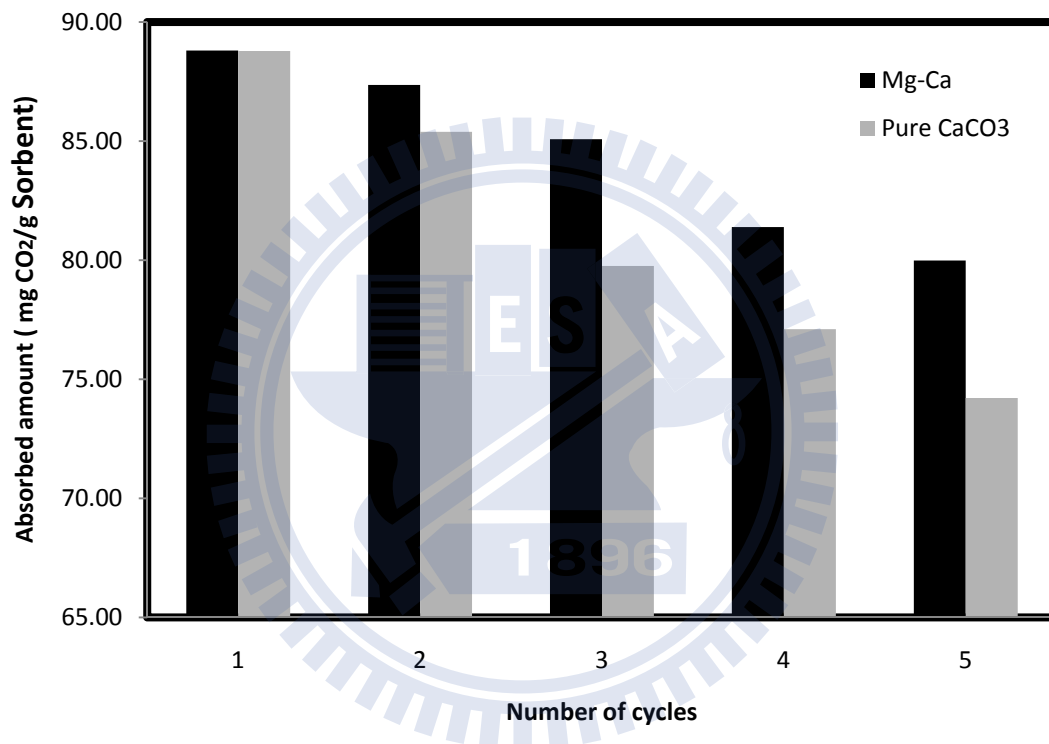
Figure 4-20 Cyclic CO$_2$ capture efficiency by packed column test. (Flow rate: 500 ccm, 15% CO$_2$, 6% O$_2$, 79% N$_2$, absorption at 700°C for 10 min, desorption at 850°C for 30 min, heating rate 36°C/min, cooling rate 6°C/min)
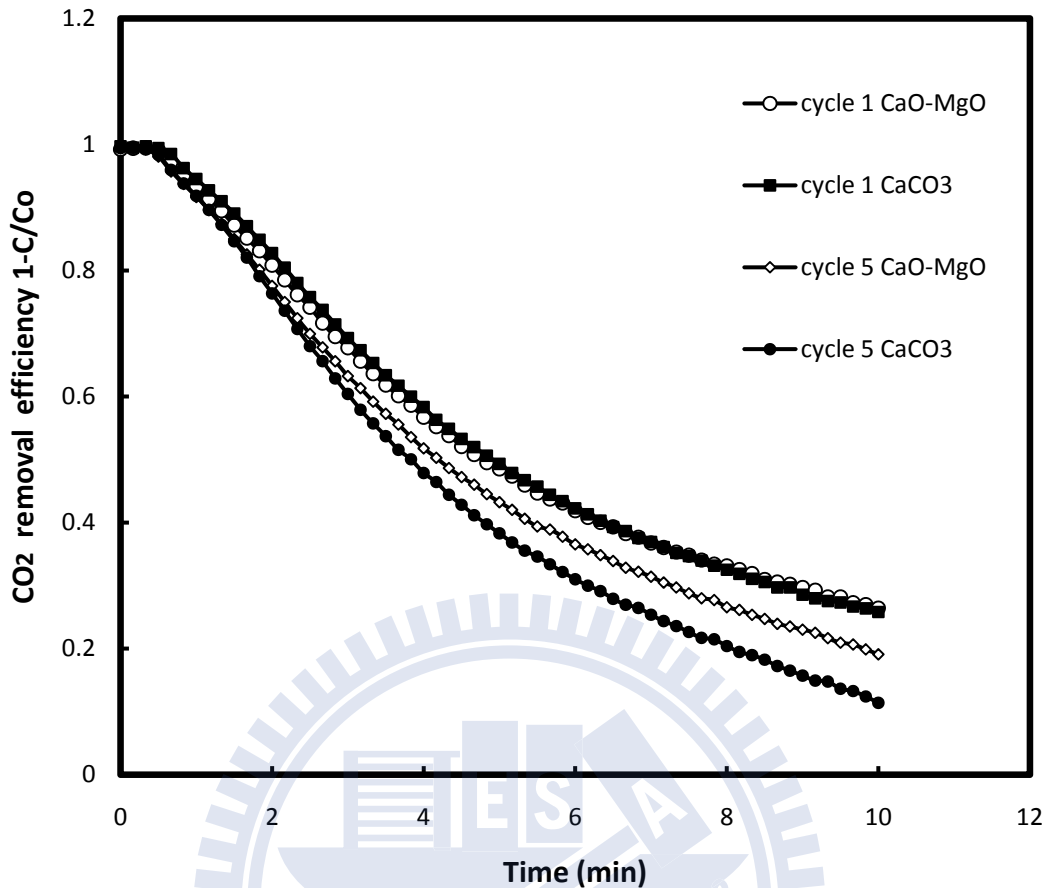
Figure 4-21 CO$_2$ removal efficiency by packed column test. (Flow rate: 500 ccm, 15% CO$_2$, 6% O$_2$, 79% N$_2$, absorption at 700°C for 10 min, desorption at 850°C for 30 min, heating rate 36°C/min, cooling rate 6°C/min)

Figure 4-22 shows the results on cyclic CO$_2$ absorbed amounts for both TGA and packed column test. At absorption temperature of 700°C and desorption temperature 850°C. The absorption time was 10 min for both system and the desorption time in packed column was 30 min, whereas it was only 1 min in the TGA test for all cycles. The absorbed amount of the CaO-MgO mixture sorbent measured in packed column system is much lower than that measured in the TGA apparatus. This is partly attributed to the effect of the heating rate in the packed column which is approximately 36°C/min without a constant rate, it means in the first minute increase from 76°C, for the second minute increase 35°C, the

66

third minutes increased 24°C so on. Also the time for the cooling rate is much longer in the packed column being this at 6°C/min exposing more the sorbent at highest temperatures. In addition, the absorption time in column test is not enough for the sorbent to reach the maximum absorbed amount in each cycle so it leads lower absorbed amounts. As well as the desorption process, this should be studied in detail, to confirm a completed desorption for every cycle, the desorption time could affect the results in the absorbed amount.
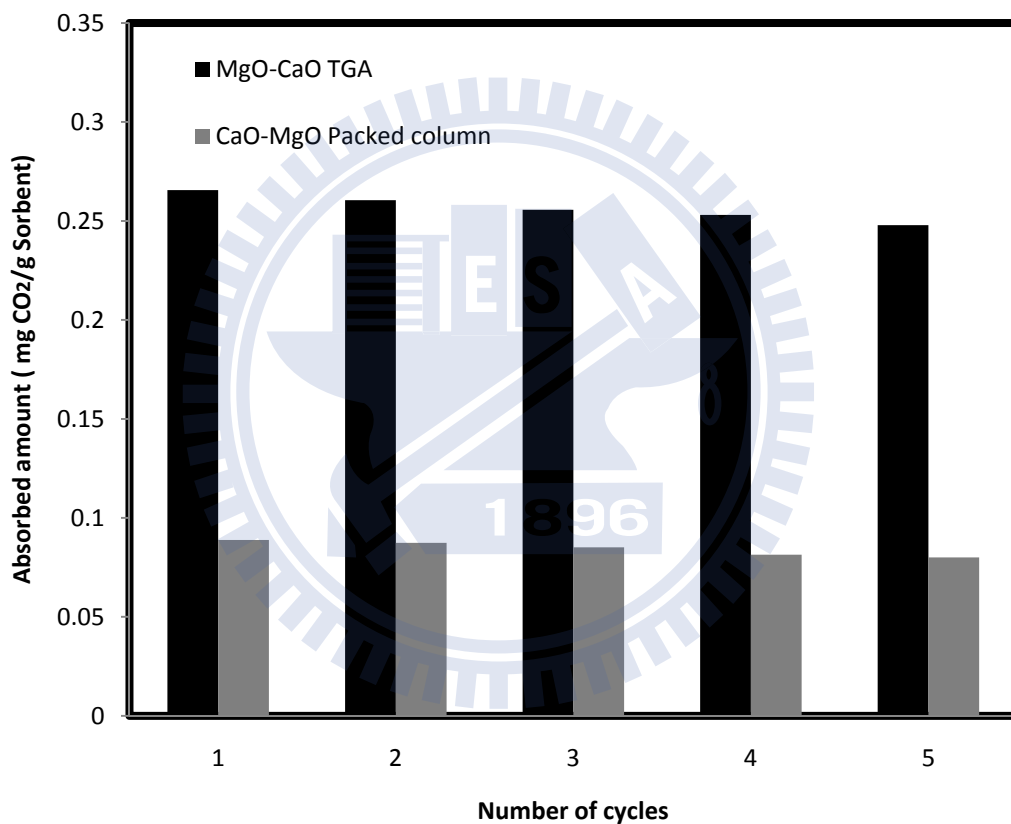
Figure 4-22 Cyclic CO$_2$ capture amounts CaO-MgO sorbent by both TGA and packed absorption column tests. The absorption time for both was 10 min.

CHAPTER FIVE CONCLUSIONS AND RECOMMENDATION

5.1 Conclusions

In this study, a TGA system was employed to find the optimal conditions for the CO_2 absorption using $CaCO_3$ precipitates as well as a mixture of CaO-MgO precipitates from sea water. From the results of this study the following conclusions can be derived:

1. The $CaCO_3$ has a range of absorption for CO_2 from 650 °C to 760°C, having a better performance at 700°C using a heating rate of 40 °C /min and cooling rate 60 °C /min.

2. Different parameters of cooling rate and heating rate were tested. If the cooling rate is lower 20°C/min the absorbed amount will increase when the CO_2 is allowed to pass since 850°C to room temperature compare to at higher cooling rate because the absorption time is longer than at 60°C/min and a the saturation of the sorbent occurs fast. The cooling rate at 20°C/min and 60°C/min seems does not affect the performance of the sorbent when there is a fixed absorption temperature of 700°C. The heating rate affects the absorption capacity of the sorbent significantly.

3. Two different conditions were tested for the absorbed amount; one is the normal process of carbonation in which the CO_2 is allowed to flow at the fixing temperature of 700°C. The other is that the CO_2 was allowed to pass during the cooling time at 850°C. It was found that more CO_2 can be adsorbed for the later one.

4. Using a mechanical mixing method between CaO (95%) and MgO (5%), a good anti- sintering sorbent can be produced. The absorbed amount was enhanced by 17% and 10% respectively, with and

without the flowing of the CO_2 during the cooling time as compared to the original CaO sorbent, while maintaining a stability of 94% and 85% after 10 cycles.

5. For the sea water precipitated CaO pure sorbent the absorbed amount was 240 mg/g for the first cycle with passing CO_2 in the cooling time, decreasing to 128mg/g after 10 cycles. For the CaO-MgO mixture sorbent, the absorbed amount was 281mg/g for the first cycle, where the CO_2 was allowed to pass during the cooling time it decreased to 266 mg/g after 10 cycles. In the case in which the CO_2 was introduce after the fixing temperature of 700°C, the absorbed amount was 266 mg/g for the first cycle, it decreased to 228 after 10 cycles.

5.2 Recommendation

1. The portion of the mixture of the $CaCO_3$ (95%) and $MgCO_3$ precipitates from sea water can be changed in order to find an optimal ratio of CaO/MgO mixture for better absorbed amount.

2. Different parameters can still be changed such as the carbonation and calcination time to study the effect in the deactivation of the sorbent.

3. At temperature programmed cooling/heating rates for the packed column can be employed to further investigation of the effect of cooling and heating on the sintering of the CO_2 absorption by CaO-MgO mixture.

REFERENCES

Abanades, J.C. and Alvarez, D. (2003). Conversion Limits in the Reaction of CO_2 with Lime. *Energy and Fuels*, 17(2), 308-315.

Abanades, J.C, G. Grasa, M. Alonso, N. Rodriguez, E. J Anthony, and L.M Romeo. (2007). Cost Structure of a Postcombustion CO_2 Capture System Using CaO. *Environmental Science and Technology*, 41(15), 5523-5527.

Abanades, Juan C., E. S. Rubin, and E.J. Anthony (2004). Sorbent Cost and Performance in CO_2 Capture Systems. *Industrial and Engineering Chemistry Research*, 43(13), 3462-3466.

Albrecht, K.O., K.S. Wagenbach, J.A. Satrio, B.H. Shanks, and T. D. Wheelock. (2008). Development of a CaO-Based CO_2 Sorbent with Improved Cyclic Stability. *Industrial and Engineering Chemistry Research*, 47(20), 7841-7848.

Alvarez, D. and Abanades, J.C., (2005). Determination of the Critical Product Layer Thickness in the Reaction of CaO with CO_2. *Industrial and Engineering Chemistry Research*, 44(15), 5608-5615.

Arakawa, H., (1998). Research and development on new synthetic routes for basic chemicals by catalytic hydrogenation of CO_2. In M. A. T. Inui and T. Yamaguchi, eds. *Advances in Chemical Conversions for Mitigating Carbon Dioxide*. Elsevier, pp. 19 - 30.

Barker, R., (1973). The reversibility of the reaction $CaCO_3$--> $CaO+CO_2$. *Journal of Applied Chemistry and Biotechnology*, 23(10), 733-742.

Benemann, J., (1997). CO$_2$ mitigation with microalgae systems. *Energy Conversion and Management*, 38, 475-479.

Bhatia, S.K. and Perlmutter, D.D., (1983). Effect of the product layer on the kinetics of the CO$_2$-lime reaction. *AIChE Journal*, 29(1), 79-86.

Borgwardt, R., (1989). Sintering of nascent calcium oxide. *Chemical Engineering Science*, 44(1), 53-60.

Botha, A., and C. A. Strydom. (2001). Preparation of a magnesium hydroxy carbonate from magnesium hydroxide. *Hydrometallurgy* 62, (3),175-183.

Butt, D.P., K. S. Lackner, C.H. Wendt, S.D. Conzone, H. Kung, Y.C. Lu, and J. K. Bremser. (1996). Kinetics of Thermal Dehydroxylation and Carbonation of Magnesium Hydroxide. *Journal of the American Ceramic Society*, 79(7), 1892-1898.

Chen, T., Neville, A. and Yuan, M., (2006). Influence of Mg2+ on CaCO$_3$ formation--bulk precipitation and surface deposition. *Chemical Engineering Science*, 61(16), 5318-5327.

Chen, Y.T., M. Karthik, and H. Bai. (2009) . Modification of CaO by Organic Alumina Precursor for Enhancing Cyclic Capture of CO2 Greenhouse Gas. *Journal of Environmental Engineering* 135, (6), 459-464.

Chrissafis, K, and K.M Paraskevopoulos. (2005b). the effect of sintering on the maximum capture efficiency of CO$_2$ using a carbonation/calcination cycle of carbonate rocks. J*ournal of thermal analysis and calorimetry.* 81(2),: 463-468.

Chrissafis, K., C. Dagounaki, and K.M. Paraskevopoulos. 2005a. the

effects of procedural variables on the maximum capture efficiency of CO_2 using a carbonation/calcination cycle of carbonate rocks. *Thermochimica Acta* 428: 193-198.

Diagne, D., Goto, M. and Hirose, T., (1995). Experimental Study of Simultaneous Removal and Concentratio of CO2 by an Improved Pressure Swing Adsorption Process. *ENERGY CONVERSION AND MANAGEMENT*, 36(6-9), 431-434.

Fang, F., Li, Z. and Cai, N., (2009a). Experiment and Modeling of CO_2 Capture from Flue Gases at High Temperature in a Fluidized Bed Reactor with Ca-Based Sorbents. *Energy and Fuels*, 23(1), 207-216.

Fang, F., Li, Z. and Cai, N., (2009b). CO_2 capture from flue gases using a fluidized bed reactor with limestone. *Korean Journal of Chemical Engineering*, 26(5), 1414-1421.

Feng, B., An, H. and Tan, E., (2007). Screening of CO_2 Adsorbing Materials for Zero Emission Power Generation Systems†. *Energy and Fuels*, 21(2), 426-434.

Freund, P., (2003). Making deep reductions in emissions from coal-fired power plant using capture and storage of CO_2. *Proceedings of the Institution of Mechanical Engineers, Part A: Journal of Power and Energy*, 217(1), 1-7.

Gabelman, A. and Hwang, S.T., (1999). Hollow fiber membrane contactors. *Journal of Membrane Science*, 159, 61-106.

Glasson, D.R., (1958). Reactivity of lime and related oxides. I. Production of calcium oxide. *Journal of Applied Chemistry*, 8(12),

793-797.

Gomes, V. and Yee, K., (2002). Pressure swing adsorption for carbon dioxide sequestration from exhaust gases. *Separation and Purification Technology,* 28(2), 161-171.

Gupta, H. and Fan, L., (2002). Carbonation−Calcination Cycle Using High Reactivity Calcium Oxide for Carbon Dioxide Separation from Flue Gas. *Industrial and Engineering Chemistry Research*, 41(16), 4035-4042.

Grasa, G.S, and J. C. Abanades. (2006). CO2 Capture Capacity of CaO in Long Series of Carbonation/Calcination Cycles. *Industrial & Engineering Chemistry Research* 45, (26), 8846-8851.

Halmann, Martin M. and Steinberg, M., (1999). *Greenhouse gas carbon dioxide mitigation*, CRC Press.

Han, C. and Harrison, D.P., (1994). Simultaneous shift reaction and carbon dioxide separation for the direct production of hydrogen. *Chemical Engineering Science*, 49(24, Part 2), 5875-5883.

Hansen, J., M. Sato, P. Kharecha, D.Beerling, R. Berner, V.M Delmotte, M. Pagani, M. Raymo, D.L. Royer, and J.C. Zachos. (2008). Target Atmospheric CO_2: Where Should Humanity Aim? *The Open Atmospheric Science Journal*, 2(1), 217-231.

Hansen, James, solomon, Dahe Q, and S. (2007).Intergovernmental Panel on Climate Change (IPCC).

Hartman, M. and Trnka, O., (2003). Calcination of calcium-based sorbents at pressure in a broad range of CO_2 concentrations. *Chemical Engineering Science*, 58(14), 3299-3300.

Hassanzadeh, A. and Abbasian, J., (2010). Regenerable MgO-based sorbents for high-temperature CO_2 removal from syngas: 1. Sorbent development, evaluation, and reaction modeling. *Fuel*, 89(6), 1287-1297.

Hendriks, C.F., (1994). *Carbon Dioxide Removal from Coal- Fired Power Plants*, Kluwer Academic Publishers.

Hu, N. and Scaroni, A.W., (1996). Calcination of pulverized limestone particles under furnace injection conditions. *Fuel*, 75(2), 177-186.

Hughes, R.W., D.Lu, E.J. Anthony, and Y.Wu. (2004). Improved Long-Term Conversion of Limestone-Derived Sorbents for In Situ Capture of CO2 in a Fluidized Bed Combustor. *Industrial & Engineering Chemistry Research* 43 (18), 5529-5539

Inui, T., M. Anpo, K. Izui, S. Yanagida, and T. Yamaguchi. (1998). *Advances in Chemical Conversions for Mitigating Carbon Dioxide*, Elsevier Science.

IPCC, (2005). *IPCC special report on carbon dioxide capture and storage*, Cambridge University Press.

Ishibashi, M, H Ota, N Akutsu, S Umeda, M Tajika, J Izumi, A Yasutake, T Kabata, and Y Kageyama. (1996). Technology for removing carbon dioxide from power plant flue gas by the physical adsorption method. *Energy conversion and management*, 37(6-8), 929-933.

Johnsen, K., H.J. Ryu, J.R. Grace, and C.J. Lim. (2006). Sorption-enhanced steam reforming of methane in a fluidized bed reactor with dolomite as CO_2-acceptor. *Chemical Engineering*

Science, 61(4), 1195-1202.

Lan, C.R. and Horng, Y.Y., (2005). Fixation of Carbon Dioxide by Carbonation with Chemical Precipitation. 12 (4).

Larson, E.D., (1993). Technology for Electricity and Fuels from Biomass. *Annual Review of Energy and the Environment*, 18(1), 567-630.

Li, L. D. L. King, Z.Nie, and C. Howard. (2009).Magnesia-Stabilized Calcium Oxide Absorbents with Improved Durability for High Temperature CO_2 Capture. *Industrial and Engineering Chemistry Research*, 48(23), 10604-10613.

Li, Z.S, N.S Cai, and Y.Y Huang. (2006). Effect of Preparation Temperature on Cyclic CO2 Capture and Multiple Carbonation Calcination Cycles for a New Ca-Based CO2 Sorbent. *Industrial & Engineering Chemistry Research* 45, no. 6: 1911-1917.

Lin, S.Y, Y. Suzuki, H. Hatano, and M. Harada. (2001). Hydrogen Production from Hydrocarbon by Integration of Water−Carbon Reaction and Carbon Dioxide Removal (HyPr−RING Method). *Energy and Fuels*, 15(2), 339-343.

Liu, W., B. Feng, Y. Wu, G. Wang, J. Barry, and João C. Diniz da Costa. (2010). Synthesis of Sintering-Resistant Sorbents for CO_2 Capture. *Environmental Science and Technology*, 44(8), 3093-3097.

Liu, W., N.W. L Low, B. Feng, G. Wang, and J. D. da Costa. (2009). Calcium Precursors for the Production of CaO Sorbents for Multicycle CO2 Capture. *Environmental Science and Technology*, 44(2), 841-847.

Lu, H., P.G. Smirniotis, F.O. Ernst, and S.E. Pratsinis. (2009).

Nanostructured Ca-based sorbents with high CO2 uptake efficiency. *Chemical Engineering Science*, 64(9), 1936-1943.

Maroto, V.M.M, Fauth D.J, Zhang Y., and Andresen J.M. (2005). Activation of magnesium rich minerals as carbonation feedstock materials for CO_2 sequestration. Available at: [Accessed May 19, (2010)].

Miliband, E., (2009). 'Clean' coal plants get go-ahead. *BBC*. Available at: http://news.bbc.co.uk/2/hi/uk_news/politics/8014295.stm [Accessed June 1, (2010)].

Mimura, T, Simayoshi, H, Suda, Iijima, M, Mituoka, and S. (1997).*Development of energy saving technology for flue gas carbon dioxide recovery in power plant by chemical absorption method and steam system*, Kidlington, ROYAUME-UNI: Elsevier.

Nakagawa, K. and Ohashi, T., (1998). A novel method of CO_2 capture from high temperature gases. *JOURNAL OF THE ELECTROCHEMICAL SOCIETY*, 145(4), 1344-1346.

Nakagawa, K. and Ohashi, T., (1998). A Novel Method of CO Capture from High Temperature Gases. *Journal of The Electrochemical Society*, 145(4), 1344-1346.

Randall M and German, (1996). *Sintering theory and practice* Wiley., New York,

Romeo, Y.L., P. Lisbona, and A. Martínez. (2009).Economical assessment of competitive enhanced limestones for CO_2 capture cycles in power plants. *Fuel Processing Technology*, 90(6), 803-811.

Ronald, B. (1974). The reactivity of calcium oxide towards carbon

dioxide and its use for energy storage. *Journal of Applied Chemistry and Biotechnology*, 24(4-5), 221-227.

Silaban, A., and D. P. Harrison. 1995. High temperature capture of carbon dioxide: Characteristics for the reversible reaction between CaO (s) and CO2 (g). *Chemical Engineering Communications* 137(1), 177-190.

Silcox, G.D., Kramlich, J.C. and Pershing, D.W., (1989). A mathematical model for the flash calcination of dispersed calcium carbonate and calcium hydroxide particles. *Industrial and Engineering Chemistry Research*, 28(2), 155-160.

Singh, D., (2003). Techno-economic study of CO_2 capture from an existing coal-fired power plant: MEA scrubbing vs. O2/CO_2 recycle combustion. *Energy Conversion and Management*, 44, 3073-3091.

Song, H., W. Cho., and Lee K., (1998). Adsorption of carbon dioxide on the chemically modified silica adsorbents. *Journal of Non-Crystalline Solids*, 242(2-3), 69-80.

Stanmore, B. and Gilot, P., (2005). Review--calcination and carbonation of limestone during thermal cycling for CO_2 sequestration. *Fuel Processing Technology*, 86(16), 1707-1743.

Symonds, R. T., D.Y. Lu, R.W. Hughes, E. J. Anthony, and A.Macchi. (2009). CO_2 Capture from Simulated Syngas via Cyclic Carbonation/Calcination for a Naturally Occurring Limestone: Pilot-Plant Testing. *Industrial & Engineering Chemistry Research* 48, (18), 8431-8440.

Takamura, Y, S Narita, J Aoki, S Hironaka, and S Uchida. (2001). Evaluation of dual-bed pressure swing adsorption for CO_2 recovery from boiler exhaust gas. *Separation and purification Technology*, 24(3), 519-528.

Vattenfall, (2008). Vattenfall and CCS – Carbon Capture and Storage Soon a Reality. Available at: http://www.vattenfall.com.

Wang, Y., Lin, S. and Suzuki, Y., (2009). Limestone Calcination with CO_2 Capture (III): Characteristics of Coal Combustion during Limestone Decomposition. *Energy and Fuels*, 23(5), 2804-2809.